# How do we see? An introduction to the biophysics of visual transduction

D.M. Horrigan[1], C.L. Makino[2]

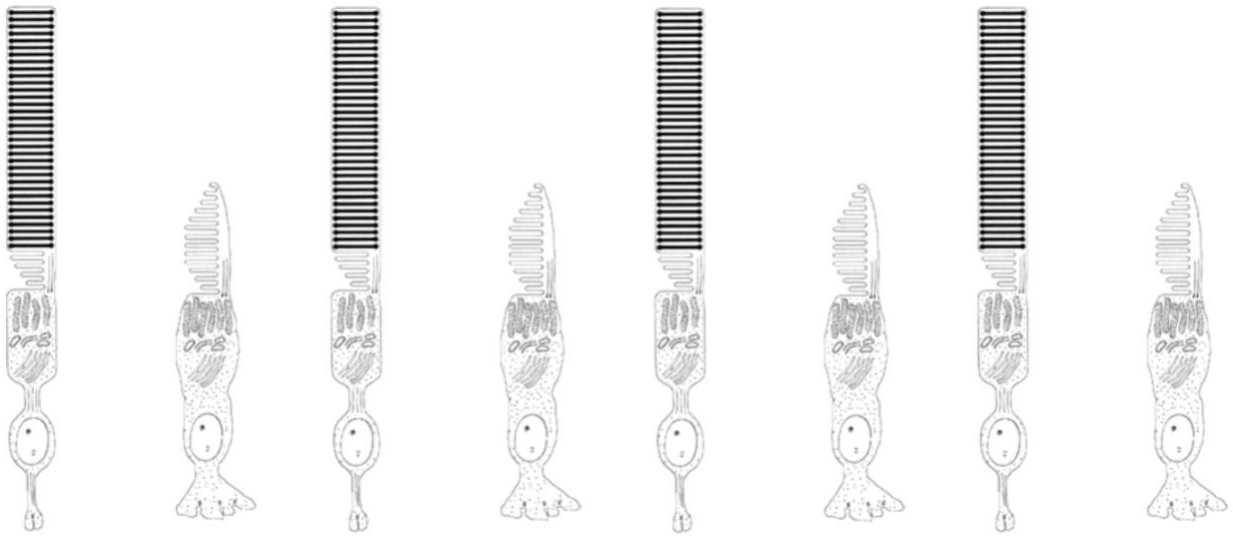


[1]Department of Pathology and Laboratory Medicine, Biology Education, Brown University, Providence, RI

[2]Department of Physiology & Biophysics, Boston University Chobanian & Avedisian School of Medicine, Boston, MA

## Introduction

For most people, the experience of seeing is such an integral part of daily life that it is difficult to imagine the complexity of the underlying processes. In this tutorial, we explain the biophysics behind the first process, visual transduction. This tutorial evolved from course lectures given at Brown University, Boston University and Harvard University. Some footnotes provide suggestions for how instructors might present the content. Hyperlinks describe the structural biology of several cascade components and/or outline biophysical approaches that advanced the field or in one case, was born from it.

Vision in very dim light calls for the ability to detect and signal single photons[1]. To accomplish such a feat, photoreceptors face a number of technical issues related to: dedication, sensitivity, timing, reproducibility and noise. These difficulties apply in general to many other signal transductions, particularly those employing a biochemical signaling cascade. As we consider each of these issues, we will discuss how Nature rose to the challenges of seeing when photons are scarce and what tradeoffs were made.

### A. Dedication

In the retina, there are cells whose sole purpose is to transduce photons into electrical signals to initiate vision. With such single-minded dedication, these photoreceptors, located in the deepest layer of the retina (**Fig. 1A**) have become highly specialized for the task. There are two types (**Fig. 1B**): cylindrically shaped rods, and the more tapered cones. In the eyes of most vertebrates, including our own, rods are more numerous.

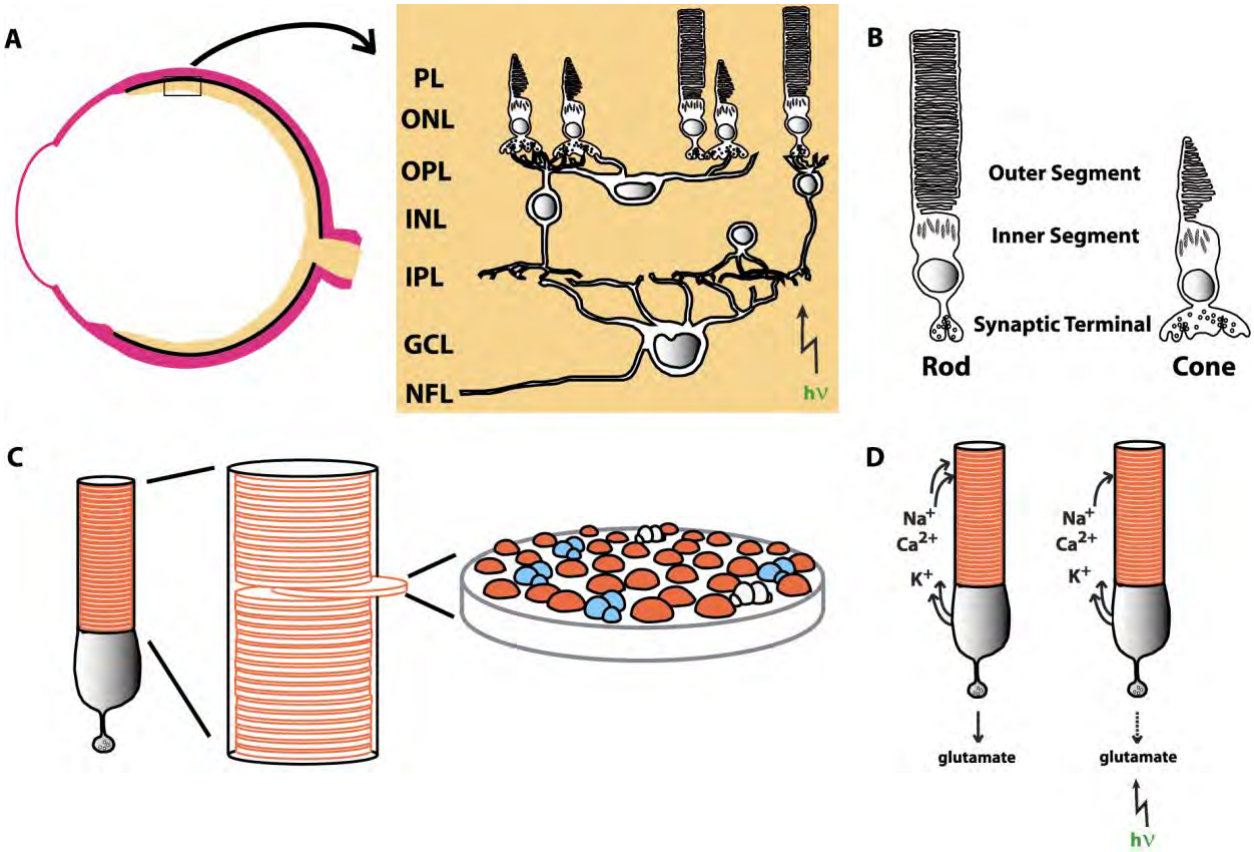


**Figure 1.** Cellular plan of vertebrate photoreceptors. **A.** Encapsulation of brain tissue, the neural retina (tan), within the vertebrate eye. The retina is laminated with various

neurons that: detect light, extract features from visual space, convey information to higher visual centers in the brain. Light passes through all layers of the retina to reach the rod and cone photoreceptors. PL, photoreceptor layer; ONL, outer nuclear layer; OPL, outer plexiform layer; INL, inner nuclear layer; IPL, inner plexiform layer; GCL, ganglion cell layer; NFL, nerve fiber layer. **B.** Morphology of rods and cones. Photons are transduced into an electrical signal in the outer segment. **C.** Rod outer segment disk membranes containing the biochemical components of the light-detecting pathway: rhodopsin (red), transducin (blue), PDE (white). **D.** The "dark" current. $Na^+$ and a lesser amount of $Ca^{2+}$ enter through cyclic nucleotide-gated channels in the outer segment while $K^+$ exits through voltage-gated channels in the inner segment. In darkness (left), the rod is depolarized and releases the neurotransmitter glutamate continuously. In response to light (right), channels in the outer segment membrane close, the rod hyperpolarizes, and glutamate release decreases. Illustrations, courtesy of Tomoki Isayama, Massachusetts Eye & Ear Infirmary and Harvard Medical School.

To provide for vision under the dimmest lighting conditions, rods have reached the pinnacle of sensitivity in that they count single photons. Cones operate under bright light. There are three kinds in our eyes, each maximally sensitive to a different wavelength. Their relative sensitivities provide the basis for color vision. Whenever you see color, the cones are in use. So, in modern society with artificial lights, vision almost never relies entirely on rods. However, if you have ever gotten up in the middle of the night to go to the bathroom and decided not to turn on the light, you may have experienced grainy, black and white images -- that is rod vision. As you can imagine, the ability to see with very little light conferred a tremendous advantage in evolution.

Rods and cones follow a similar blueprint in all vertebrates. They are unipolar, elongated neurons that act as waveguides, to better sample a specific part of visual space. Rods and cones can be divided into two portions, termed inner segment (IS) and outer segment (OS), according to their radial positions within the retina (**Fig. 1A,B**). The inner segment consists of the cell body and contains the cellular organelles found in other neurons. A synaptic terminal is filled with vesicles containing neurotransmitter. Vesicular release is regulated by voltage-gated $Ca^{2+}$ channels in the plasma membrane. The outer segment is a non-motile cilium that functions as the light transducing organelle. It contains a stack of nearly a thousand hollow membranous disks and all of the components of the phototransduction enzyme cascade (**Fig. 1C**). In rods, the disks are enclosed by the plasma membrane of the outer segment, whereas in cones, the disk membranes are an extension of the plasma membrane arranged into a series of evaginations that are open to the extracellular space (**Fig. 1B**).

### B. Sensitivity/Amplification

According to physical law, in order for light to have an effect, it must first be absorbed. The corollary for our purposes is that in order for light to be seen, it must be absorbed by the visual pigment, rhodopsin. Rhodopsin consists of 2 parts. One part is the chromophore or "color bearer" that absorbs the light, the other part is a protein called opsin. The chromophore is 11-*cis* retinal, which is covalently linked to the opsin at lysine at position 296, within H7, the seventh transmembrane helix (**Fig. 2A**).

Retinal is the oxidized or aldehyde form of vitamin A, which cannot be made *de novo* by the body; it must be taken in constantly in the diet. Hence, vitamin A deficiency leads to depletion of 11-*cis* retinal necessary to form rhodopsin and night blindness -- recall that rods do the heavy lifting during low light situations. 11-*cis* Retinal is a hydrocarbon with a cyclohexene ring connected to a chain of carbons linked with alternating double and single bonds (**Fig. 2C**). This

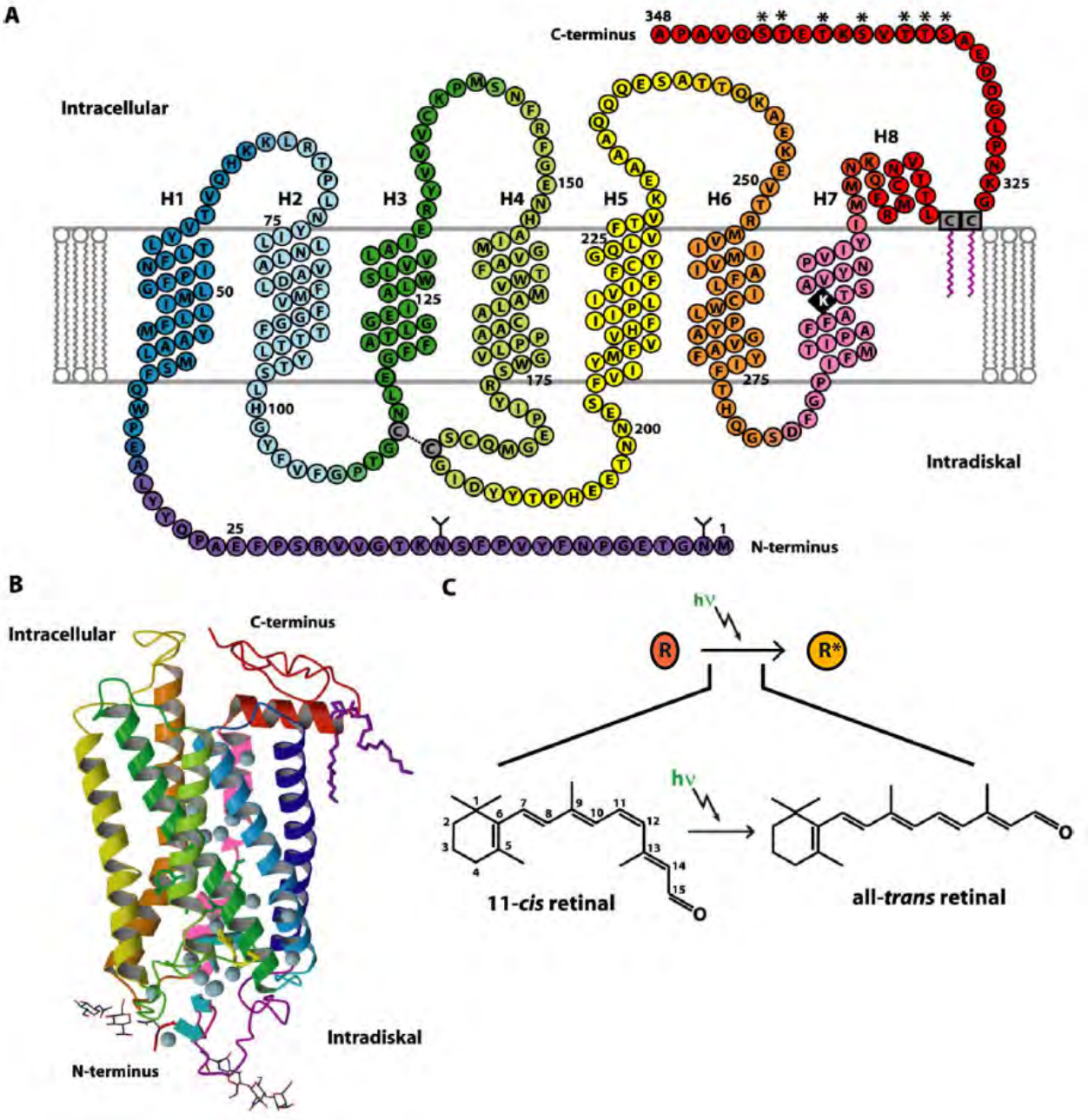


**Figure 2.** Structure of rhodopsin. **A.** Amino acid sequence of bovine opsin. The glycosylated N-terminus (violet residues) is located within the outer segment disk (intradiskal space) or in the extracellular space for rhodopsins in the plasma membrane, while the C-terminus (red residues) is exposed to the cytoplasm, with the seven $\alpha$-helices (H1-H7) spanning the membrane. There are seven phosphorylation sites (*, human rhodopsin only has six phosphorylation sites) and two palmitoylated cysteines (gray squares) on the C-terminus. Two conserved cysteines (gray circles) on the first and second extracellular loops form a disulfide linkage on the intradiskal side. The retinal chromophore binds as a protonated Schiff base to K296 (black diamond). **B.** X-ray crystal structure of bovine rhodopsin. The color scheme for the helices (H1-H8) corresponds to that in **A**. The blue spheres represent water molecules, and the arrows indicate β-strand structure. Figure, courtesy of Tetsuji Okada, Gakushuin University. **C.**

The retinal chromophore of rhodopsin. Photoisomerization of the 11-*cis* retinal in opsin's chromophore-binding pocket to the all-*trans* conformation transforms rhodopsin to the activated state (R*). Illustrations in **A** and **C**, courtesy of Tomoki Isayama, Massachusetts Eye & Ear Infirmary and Harvard Medical School.

bonding scheme between carbons is special because the bonds are not true double or single bonds, they are something in between and the electrons responsible for forming these so-called $\pi$ bonds are no longer tied to the carbon of origin. Instead, the $\pi$ electrons roam over all carbons in the conjugated system and with this high degree of freedom, it takes relatively little energy to raise them to the excited state (**Fig. 3**). Capture of a photon by rhodopsin causes an isomerization, changing the bent, 11-*cis* retinal to a straight, all-*trans* conformation (**Fig. 2C**). Because the retinal is covalently bound to the opsin and enveloped by its helices, the change in chromophore shape pushes against the protein, converting the dark-adapted, inactive form to the light-activated R*. Light literally flips a molecular switch!

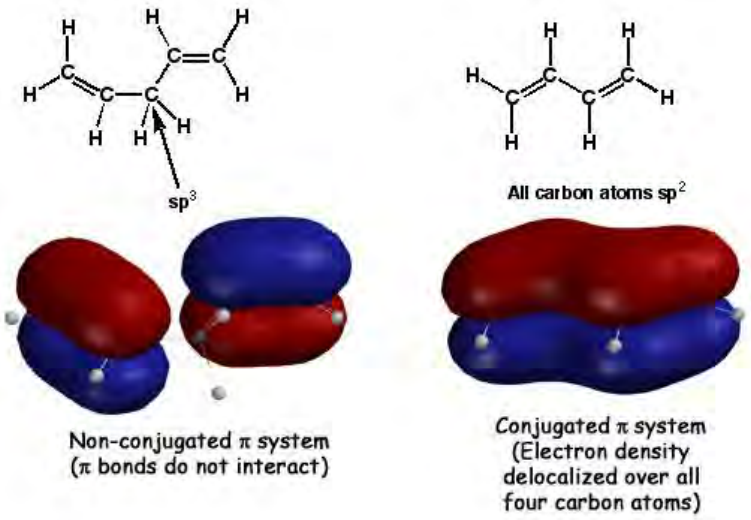


**Figure 3.** Localized vs delocalized bonding electrons. Illustration, courtesy of Brent Iverson, University of Texas Austin.

Opsin is an integral membrane protein consisting of a single polypeptide chain of 348 amino acids (**Fig. 2A**). Knowing the amino acids makes it possible to infer secondary structure of the protein. Hydrophobicity analysis, along with antibody binding studies, made it clear that rhodopsin had seven helical segments that crossed the membrane, making rhodopsin the founding father of what has come to be known as the seven-transmembrane-helix receptor or 7TM receptor family of receptors, the most diverse receptor family in Nature. This is great news for students and scientists alike, because it means that the lessons learned in visual transduction apply to many other systems which utilize 7TM receptors, including olfaction, some forms of taste, hormone response, some forms of neurotransmission and even other signal transductions for cytokines, peptides, ions, etc. outside the nervous system. Rhodopsin was also the first 7TM receptor to have its X-ray crystal structure solved (**Fig. 2B**), affording visualization of the protein's structure at atomic resolution.

Strictly speaking, opsin is the 7TM receptor and 11-*cis* retinal is the ligand (an inverse agonist). Rhodopsin is the name given to opsin with 11-*cis* retinal bound. Rhodopsin and related pigments are the only 7TM receptors that get a special name for the ligand-bound state. But rhodopsin deserves a special name because it is the only 7TM receptor that binds its ligand covalently and because the interaction between opsin and 11-*cis* retinal to form visual pigment is collaborative. 11-*cis* Retinal by itself absorbs high energy, UV light. But in rhodopsin, the

opsin protein rearranges the electrons within 11-*cis* retinal, lowering the energy requirement and shifting absorption to 500 nm, which on the electromagnetic spectrum is blue-green light (**Fig. 4**). In cone pigments, the chromophore is surrounded by different amino acid residues that tune the chromophore's absorption to other wavelengths. Retinal has an extinction coefficient (which is a measure of how well a molecule absorbs light at a given wavelength) of 25,000-30,000 $M^{-1}$ $cm^{-1}$ at $\lambda_{max}$, which is pretty good, but opsin makes it even better, raising it to 42,000 $M^{-1}$ $cm^{-1}$. Retinal has a preferred axis for light absorption, that is, when its long axis is parallel to the electric vector of the light. In the rod, rhodopsin orients the 11-*cis* retinal so that its "good" side faces the incoming light to maximize the probability of photon capture.

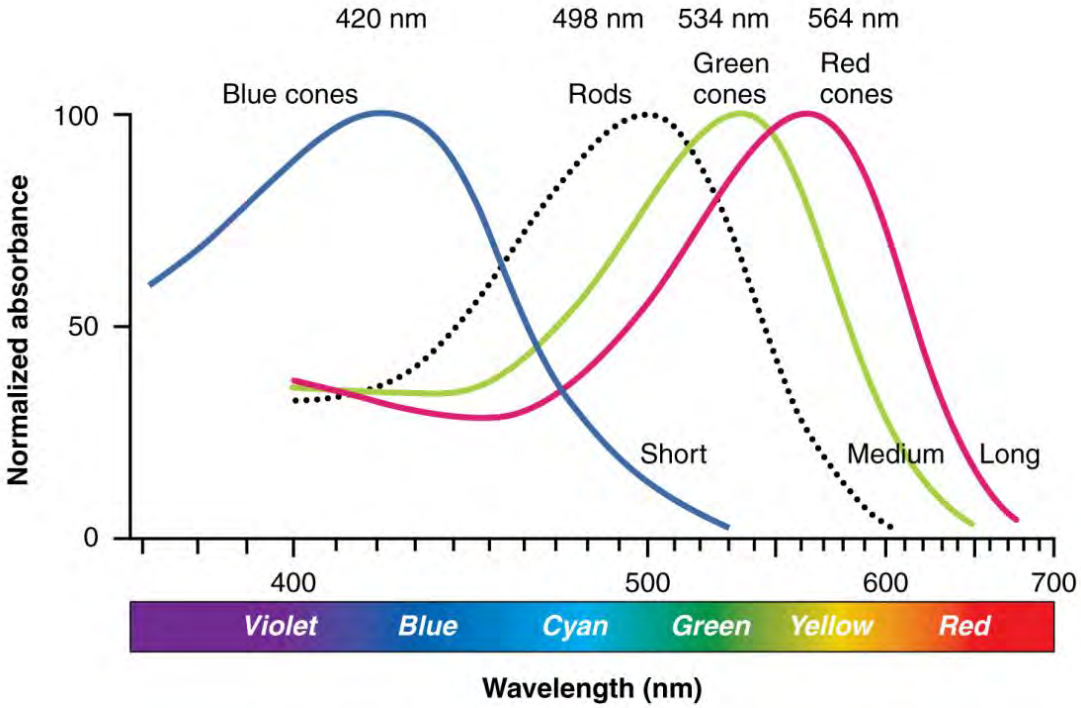


**Figure 4.** Absorbance spectra of visual pigments. Opsins shift the positions of the π electrons in 11-*cis* retinal, tuning the chromophore's absorption to different peak wavelengths of light in the blue, blue-green, green or yellow. Image Credit: Anatomy & Physiology, Connexions, http://cnx.org/content/col11496/1.6/, licensed under CC BY 3.0.

In order to capture a lot of photons, a lot of rhodopsin is needed. It follows that since rhodopsin is a membrane protein, a lot of membrane is needed. That is why the rod outer segment contains so many disks -- the disks supply the membrane (**Fig. 1**). The long axis of the outer segment points to the pupil, so a photon entering the eye attempts to zip past all of the rhodopsins as it passes sequentially through the disks[2]. A human rod contains about two hundred million molecules of rhodopsin packed in one thousand disks. About a third of the photons pass through all of the disks and cannot be seen; the rest are absorbed by rhodopsins. Photon capture is a key determinant of the sensitivity of the system, so one way to improve sensitivity would be to increase the number of disks in the outer segment, making it more likely that the photon gets absorbed. Optical density (OD) of the outer segment obeys the Beer-Lambert Law:

$$OD = \varepsilon c l, \quad (1)$$

where $\varepsilon$ is the extinction coefficient characteristic of rhodopsin, $c$ is the rhodopsin concentration and $l$ is the pathlength that the photon must take (related to the number of disks). Frogs and toads have rod outer segments that are roughly twice as long as those of humans with twice the number of disks, so nine out of ten photons are absorbed. Some deep-sea fish have rod outer segments that are about seven times longer than ours and they essentially catch every photon.

Having captured a photon, the rod sets out to amplify the signal to ensure that it stands out against any background noise. One of Nature's strategies for amplification is a biochemical cascade in which there are nested reactions with the product of each reaction catalyzing a subsequent reaction (**Fig. 5**). Greater amplification is achieved by increasing the number of nested reactions and by extending the duration of the cascade operation. A G protein cascade is used for visual transduction.

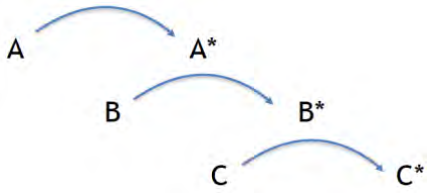


**Figure 5**. A biochemical cascade. A is inactive while A* activates the conversion of B to B* and B* activates the conversion of C to C*.

Many, but not all 7TM receptors are coupled to G proteins and are known as G protein-coupled receptors (GPCRs). In fact, GPCRs are one of the major protein targets of the pharmaceutical industry, and many drugs on the market block (or in some cases activate) GPCRs. G proteins are intracellular heterotrimeric proteins, consisting of $\alpha$-, $\beta$-, and $\gamma$-subunits. Some rhodopsin-like pigments participate in signal transductions that do not need a lot of amplification and they are not GPCRs (**Hyperlink 1: Channelrhodopsins and optogenetics**). All visual pigments are GPCRs, however. Transducin is the G protein in rods and cones that interacts with rhodopsin (**Fig. 6A**). In its inactive state, the $\alpha$-subunit of transducin (T$\alpha$) has a GDP bound to it. Photoisomerization of rhodopsin transforms it into an active state, R*, that acts as a GEF (guanosine nucleotide exchange factor). R* binds transducin and releases the GDP bound to the $\alpha$-subunit (**Hyperlink 2: Activations of rhodopsin and transducin**)**.** Another GDP could bind, but a GTP is more likely to do so because its concentration inside the rod is higher than that of GDP. Upon GTP binding, transducin dissociates from R* and the $\beta\gamma$-subunits dissociate from the $\alpha$-subunit (**Fig. 6B**). In some systems, the $\beta\gamma$-subunits act on a channel or some other downstream effector. In rods, T$\beta\gamma$ is not known to do anything with regard to phototransduction except to help T$\alpha$ bind R*. R* repeats this action over and over, effectively amplifying the signal, until its activity is shut off. Transducin serves as an intermediary between R* and a downstream effector, PDE6 (phosphodiesterase type 6, hereafter referred to simply as PDE), an enzyme that cleaves the phosphodiester bond of cGMP to convert it to 5'-GMP and a $H^+$. PDE is a heterotetramer that consists of a dimer of two catalytic protein subunits, PDE$\alpha$ and PDE$\beta$, each with an active site inhibited by a PDE$\gamma$-subunit. Activated T$\alpha$-GTP binds to PDE$\gamma$ to relieve the inhibition on a PDE catalytic subunit (**Fig. 7**, left), but the binding of one T$\alpha$-GTP does not have a significant impact on the activity of PDE. Only when two T$\alpha$-GTP subunits bind does PDE become fully active (**Hyperlink 3: PDE structure and cryo-EM**).

So far, all of the action has taken place on the disk membrane (**Fig. 7**, left) that is completely internalized in rods. A small, soluble molecule, cGMP, links the action on the disks to the ion

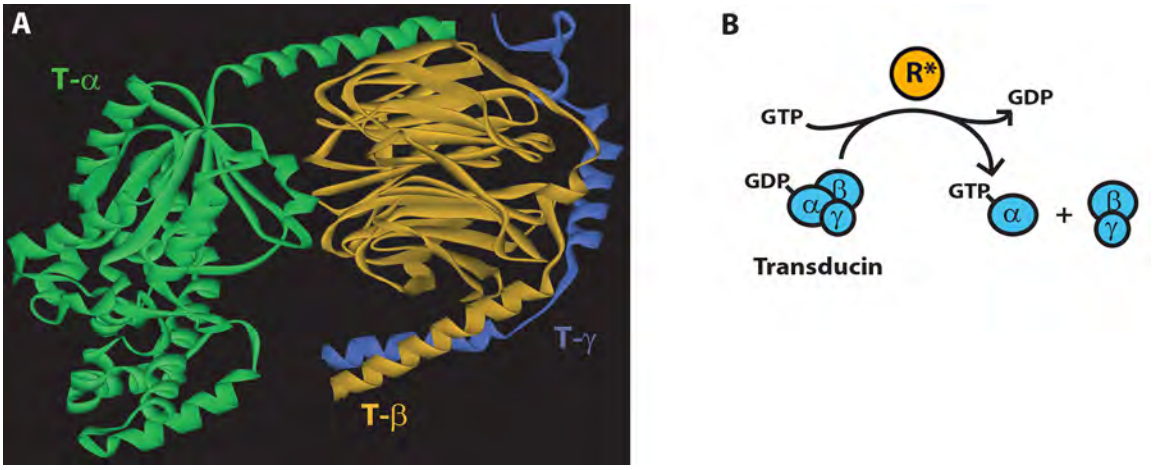


**Figure 6**. Structure of transducin. **A.** Heterotrimeric composition of transducin. Figure, courtesy of Kirill Martemyanov, Scripps Research Institute Florida. **B.** Activation of transducin. R* binds the transducin heterotrimer and catalyzes the exchange of a GTP for a GDP bound to Tα, leading to the release of the transducin and the separation of the Tα-GTP from Tβγ. Illustration, courtesy of Tomoki Isayama, Massachusetts Eye & Ear Infirmary and Harvard Medical School.

channels on the plasma membrane. When PDE is active, the cGMP concentration within the outer segment decreases, and cyclic nucleotide-gated (CNG) ion channels respond by closing (**Fig. 7**, right) . The discovery that these ion channels were gated directly by cGMP was a revelation in biology, because until that time people thought that cyclic nucleotides elicited their effects through the phosphorylation of proteins. CNG channels are now widely studied in other neurons, as well as in kidney, heart and other organs. With cGMP bound, the pore is open. When cGMP comes off, the interactions within the channel holding the pore open are weakened or disrupted completely and that causes the channel to close (**Hyperlink 4: CNG channel gating**).

In textbook descriptions of the nervous system, neurons are hyperpolarized at rest and stimulation opens cation channels that leads to depolarization causing in many cases, an action potential. At the synapse, depolarization opens voltage-gated calcium channels, followed by vesicle fusion at the membrane to release neurotransmitter. Rods and cones work in the exact opposite way! In darkness, a circulating or “dark” current due to the open CNG channels depolarizes the photoreceptor and sustains neurotransmitter release at the synapse. Stimulation by light *closes* the CNG channels, *hyperpolarizes* the photoreceptor and *decreases* neurotransmitter release at the synapse (**Fig. 1D**)[3].

How much amplification is achieved? In other words, when one photon is captured by one rhodopsin, how many downstream molecules are activated (**Fig. 8A**)? Once R* activates a transducin, that transducin falls off, so the same R* can activate another and another transducin. Estimates for the number of transducins activated per R* range from many tens to a few hundred, so there is amplification at this step.

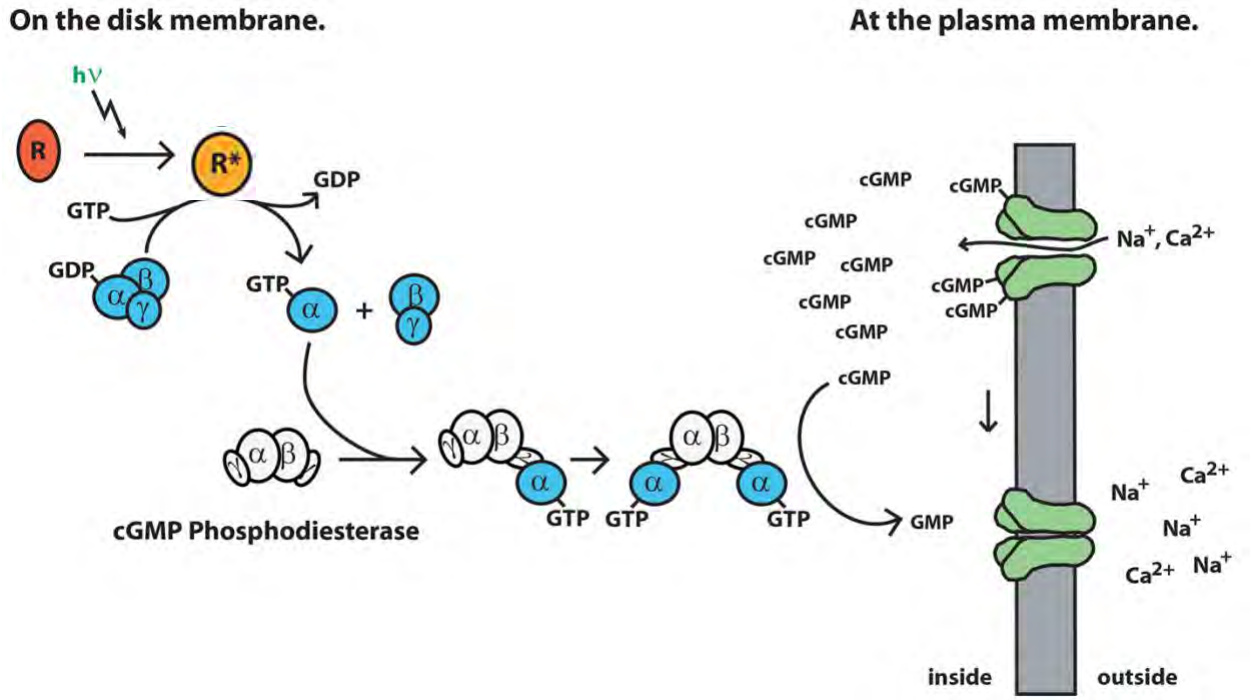


**Figure 7.** Bridging the gap between photon absorption at the disk membrane and channel closure at the plasma membrane. On the disk membrane (**left**), photoisomerization of rhodopsin (R) transforms it to the active state of the pigment (R*). R* catalyzes the transfer of a GTP for the GDP bound to transducin (blue), causing the βγ-subunits to come off, making Tα-GTP available to activate phosphodiesterase (PDE, white). A Tα-GTP can bind one PDEγ-subunit, but two Tα-GTPs are needed to activate the PDE catalytic subunits (PDEα and PDEβ). Activated PDE hydrolyzes cGMP, the intracellular messenger that is required for the CNG channels (green) in the outer segment plasma membrane to remain open (**right**). Reduction in the intracellular levels of cGMP closes channels, blocking entry of $Na^+$ and $Ca^{2+}$ and thereby decreasing the dark current. Illustrations, courtesy of Tomoki Isayama, Massachusetts Eye & Ear Infirmary and Harvard Medical School.

It takes two Tα-GTP to relieve the inhibition on PDE, so some amplification is lost at this step (**Fig. 8B**), but as will be justified below, for good reason. In total, ten or perhaps as many as a few tens of PDE dimers are activated per photoisomerization.

PDE is a powerful enzyme; with a $k_{cat}/K_m > 10^8\ M^{-1}\ s^{-1}$, it hydrolyzes cGMPs as fast as it encounters them (**Fig. 8B**) . An enzyme that functions this quickly is said to be diffusion limited. Obviously, there is amplification at this step.

Additional amplification comes from the way in which the channel responds to changes in cGMP concentration. The dose-response curve for the channel (current versus concentration of cGMP) follows the Hill equation (**Fig. 8D**)[4]:

$$I/I_{max} = cGMP^n/(cGMP^n + K_{0.5}^n), \qquad (2)$$

where $K_{0.5}$ is the concentration at which half the channels are open and n is the Hill coefficient. When n>1, there is cooperativity, that is, the binding of one cGMP enhances additional binding

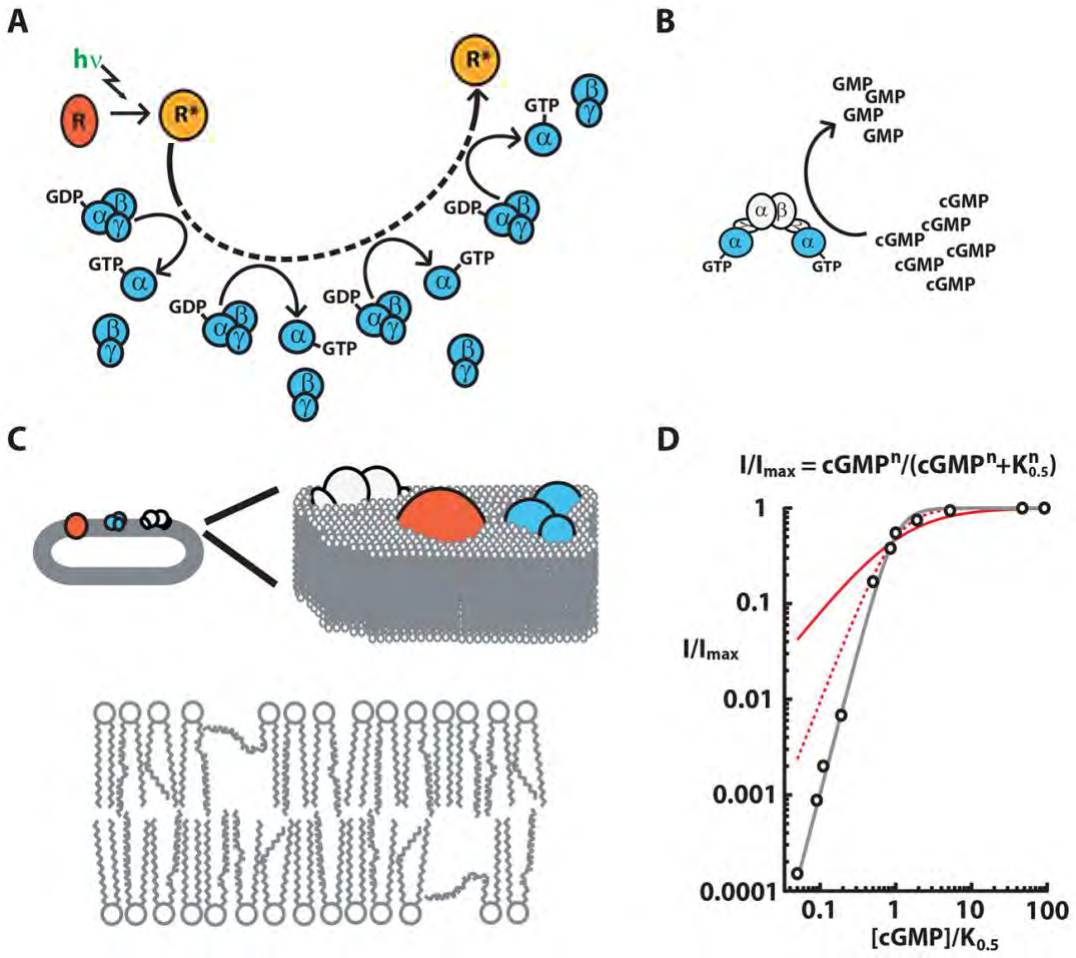


**Figure 8.** Amplification in the phototransduction cascade. **A.** Rhodopsin catalysis of transducin activation. A single R* sequentially activates many transducins. **B.** Enzymatic activity of PDE. With two T$\alpha$-GTPs bound, PDE hydrolyzes cGMP at the diffusion limit. **C.** Protein interaction on the disk membrane. Transduction is improved by anchoring R (red), transducin (blue), and PDE (white) to the phospholipid bilayer to ensure timely collisions (upper). The high unsaturated fatty acid content of the disk membrane makes them very fluid because double bonds introduce kinks that disrupt the tight, orderly packing of the fatty acids (lower). **D.** Cooperativity of CNG channel gating. Channel opening increases as the third power of cGMP concentration. For comparison, solid and dashed red lines depict the dose-response relations with Hill coefficients of n=1 and n=2, respectively. More channels are open at a given [cGMP] below the $K_{0.5}$, but changes in cGMP levels produce less dramatic effects. Illustrations, courtesy of Tomoki Isayama, Massachusetts Eye & Ear Infirmary and Harvard Medical School.

and channel opening. For the native channel, n is about 3 (**Fig. 8D,** gray line). The minimal amount of cGMP that must be present to open the channel is high, but channel opening is very sensitive to changes in cGMP. Put another way, cooperativity turns the channel into a biological switch; it tends toward populating the channel either in the open state with a full complement of cGMP molecules bound or in the closed state without any cGMP molecules bound. Therefore, the signal transduced by the disk membrane-bound components is further amplified at the

plasma membrane by the cooperative nature of cGMP binding to the channel. Ultimately, a single photon closes hundreds of channels and thereby prevents the entry of about a million $Na^+$ ions into the rod. *Amplification is a millionfold***.**

**C,D. Timing and Reproducibility**

The next two issues, timing and reproducibility, are intertwined and will be considered together. Photon absorption isomerizes the 11-*cis* retinal to all-*trans* retinal with blazing speed -- it only takes a few hundred femtoseconds. This discovery caused quite a stir at the time, because nuclear rearrangements were thought to occur on a much slower time scale. At first glance, one might think it has been overengineered. After all, in dim light, we might be able to see flicker at 15 Hz or flashes separated by about 70 ms, a far cry from hundreds of femtoseconds. So why so fast? The answer is -- reliability**[5]**.

Energy could dissipate by fluorescence or heat as the rhodopsin collides with other molecules, but since isomerization occurs a trillion times faster than the blink of an eye ($10^{-13}$ s for isomerization vs $10^{-1}$ s for an eyeblink), there is virtually no opportunity for slower things to happen. The quantum efficiency of isomerization, that is the probability of rhodopsin isomerizing once it has absorbed a photon is 0.7, which is pretty high. It takes longer to rearrange opsin, about a millisecond, which is still fast, just not blazing fast.

In a biochemical cascade, amplification takes time. To reduce the transduction delay imposed on vision, subsequent cascade steps responsible for initiating the photon response incorporate features designed for maximizing speed. Transducin and PDE join rhodopsin on the disk membrane. Reduction of the reaction space from a three-dimensional volume (aqueous cytoplasm) to a two-dimensional surface (disk membrane) increases the collision rates and allows for the orientation of each protein to be optimized to favor the forward reaction (**Fig. 8C**).

Two-dimensional is good, but viscous membranes slow the motion of proteins. To minimize this problem, rod membranes contain a very high concentration of long, unsaturated fatty acids which confer disorder and hence, fluidity. Long, straight, fatty acids pack tightly and form a stiff membrane, but kinked chains of unsaturated fatty acids leave pockets of space in which the fatty acid chains can jiggle (**Fig. 8C**) and proteins can move about more freely. As a result, disk membranes have a consistency like olive oil. With a viscosity of about 1 poise, they are among the most fluid membranes in the body. This fluidity allows R* to collide with and activate about a thousand transducins per second.

To get the CNG channel to respond quickly to a fall in cGMP, it must have a low affinity for cGMP. Otherwise, the channel would not readily release a bound cGMP after a drop in intracellular cGMP concentration. The CNG channel in rods has a fairly high Michaelis constant ($K_m$) of tens of micromolar. The cGMP concentration in the cell is just a few micromolar, so only a small fraction of the channels are open. Then in order to have a significant dark current, the rod expresses a lot of CNG channels, for which there are consequences, discussed below.

For response shutoff, timing is critical for setting photoresponse amplitude, duration, and reproducibility. R* in rods will shut itself off by undergoing a thermal transition, but it could take minutes at body temperature. This is much too slow to be useful, but if it were too fast, R* could shut off before activating any transducins. Besides the slow timing, there is another problem. A stochastic, random process has an exponential distribution; some R* will shut off with little delay and give rise to small single photon responses, while others will shut off with a long delay and give rise to large responses. To speed things up, rods call on arrestin to bind R* (**Fig. 9A**). Arrestin is a very large, soluble protein, whose sheer bulk prevents transducins from getting

close enough to bind R* (**Fig. 10**). The solution to premature shutoff and random timing associated with stochasticity is to arrange for a multi-step shutoff process. Human rhodopsin has six (bovine rhodopsin has seven, **Fig. 2A**) serines and threonines on the carboxy terminus that are targeted for phosphorylation by the enzyme rhodopsin kinase (GRK1). Each added phosphate simultaneously reduces the rate of transducin activation by R* and increases its affinity for arrestin binding. Typically, R* binds arrestin, which completely quenches the activity, after two sites are phosphorylated.

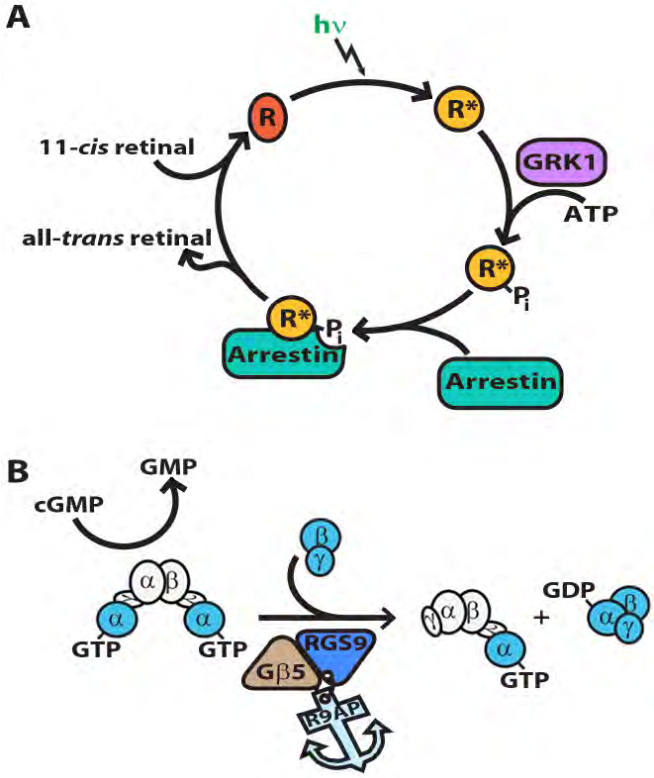


**Figure 9.** Inactivation of the cascade. **A.** Shutoff of R*. Phosphorylation of R* by rhodopsin kinase (GRK1) decreases transducin activation, but binding to arrestin is necessary to completely quench its activity. All-*trans* retinal comes off and a new 11-*cis* retinal binds the opsin to regenerate rhodopsin. **B.** Shutoff of transducin and PDE. Transducin is inactivated upon its hydrolysis of the bound GTP to GDP. The slow, intrinsic GTPase activity of transducin is accelerated by a complex consisting of RGS9, Gβ5, and R9AP. Upon hydrolysis of GTP to GDP, Tα releases PDEγ that then re-inhibits PDE. Tα-GDP eventually combines with Tβγ to reconstitute the inactive heterotrimer. Illustrations, courtesy of Tomoki Isayama, Massachusetts Eye & Ear Infirmary and Harvard Medical School.

Transducin has an intrinsic GTPase activity. After hydrolyzing GTP to GDP, transducin releases PDEγ. So transducin not only couples R* to PDE, it is a timer for PDE activity (**Fig. 9B**). Transducin's GTPase activity takes many seconds which again, is too slow. However, there is a heterotrimeric GAP (GTPase accelerating protein) complex that advances the timing of GTP hydrolysis by more than tenfold. In rods and cones, the GAP complex consists of RGS9 (regulator of G protein signaling type 9), Gβ5 (a "G protein β-subunit" that never actually forms a heterotrimeric G protein), and R9AP (RGS9 anchoring protein that affixes the GAP complex to the disk membrane) (**Fig. 11**). To ensure that transducin does not shut off before

activating PDE, T$\alpha$-GTP and the GAP complex have a low affinity for binding. However, the affinity of the GAP complex is high for T$\alpha$-GTP bound to PDE$\gamma$.

**Figure 10.** Steric capping of R* (gold) by arrestin (teal). The connection of the phosphorylated C terminus of rhodopsin to helix VII is not resolved. Figure, courtesy of Vsevolod Gurevich, Vanderbilt University. Adapted from Zhou, X.E., He, Y., de Waal, P.W., Gao, X., Kang, Y., Van Eps, N., Yin, Y., Pal, K., Goswami, D., White, T.A., Barty, A., Latorraca, N.R., Chapman, H.N., Hubbell, W.L., Dror, R.O., Stevens, R.C., Cherezov, V., Gurevich, V.V., Griffin, P.R., Ernst, O.P., Melcher, K., and Xu, H.E. 2017. Identification of phosphorylation codes for arrestin recruitment by G protein-coupled receptors. Cell 170: 457-469. Copyright 2017, Elsevier Inc.

Full recovery requires that the intracellular cGMP concentration be restored to dark-adapted levels so that the CNG channels can reopen. Cyclic GMP is synthesized continuously from GTP by membrane guanylate cyclases. In darkness, synthesis of cGMP is restrained by the action of GCAPs (guanylate cyclase activating proteins). One GCAP is bound to each subunit, preventing full activity (**Fig. 12B**). Thus, recovery could take a pretty long time if it were to rely on the slow, basal rate of cyclase activity. The rod, however, has an engineering solution -- feedback!

The feedback is based on $Ca^{2+}$ (**Fig. 12**). $Ca^{2+}$ enters the rod through the CNG channels and is extruded by a $Na^{+}/K^{+},Ca^{2+}$ exchanger protein in the outer segment plasma membrane. This exchanger is special in that it couples $Ca^{2+}$ extrusion to two ion gradients: $Na^{+}$ entering and $K^{+}$ exiting, enabling it to efficiently drive internal $Ca^{2+}$ down to a very low level. Closure of CNG channels stops $Ca^{2+}$ entry and continuous removal by the exchanger gives rise to a light-induced fall in intracellular $Ca^{2+}$ (**Fig. 12A**). With bright light that closes all of the channels, intracellular $Ca^{2+}$ concentration drops by an order of magnitude. The fall in $Ca^{2+}$ is sensed by the GCAPs. GCAPs inhibit guanylate cyclase when they have $Ca^{2+}$ bound, but when internal $Ca^{2+}$ drops, $Ca^{2+}$ ions dissociate from GCAPs allowing $Mg^{2+}$ ions to bind in their place. With $Mg^{2+}$ bound, GCAPs stimulate guanylate cyclase to make cGMP at a severalfold faster rate (**Fig. 12B,C**). The CNG channel is a second target for feedback. In the dark, $Ca^{2+}$/calmodulin (or a related protein in cones) binds the channel and reduces its affinity for cGMP (**Fig. 12D**). When internal $Ca^{2+}$ falls, calmodulin abandons the CNG channel and it will now open at a lower concentration of cGMP. Bottom line? The single photon response in rods recovers in a timely manner and is very reproducible, with a coefficient of variation (ratio of SD/mean) of approximately 0.2.

### E. Noise

At all temperatures above absolute zero, molecules are in constant motion, fidgeting and banging into each other. Inactive rhodopsin (R) with covalently bound 11-*cis* retinal, does not activate transducin. But every now and then, an R can accumulate sufficient internal energy that enables 11-*cis* retinal to thermally isomerize in the absence of a photon. Rhodopsin is incredibly stable, however, with a half-life for thermal isomerization at mammalian body temperature of 400 years!

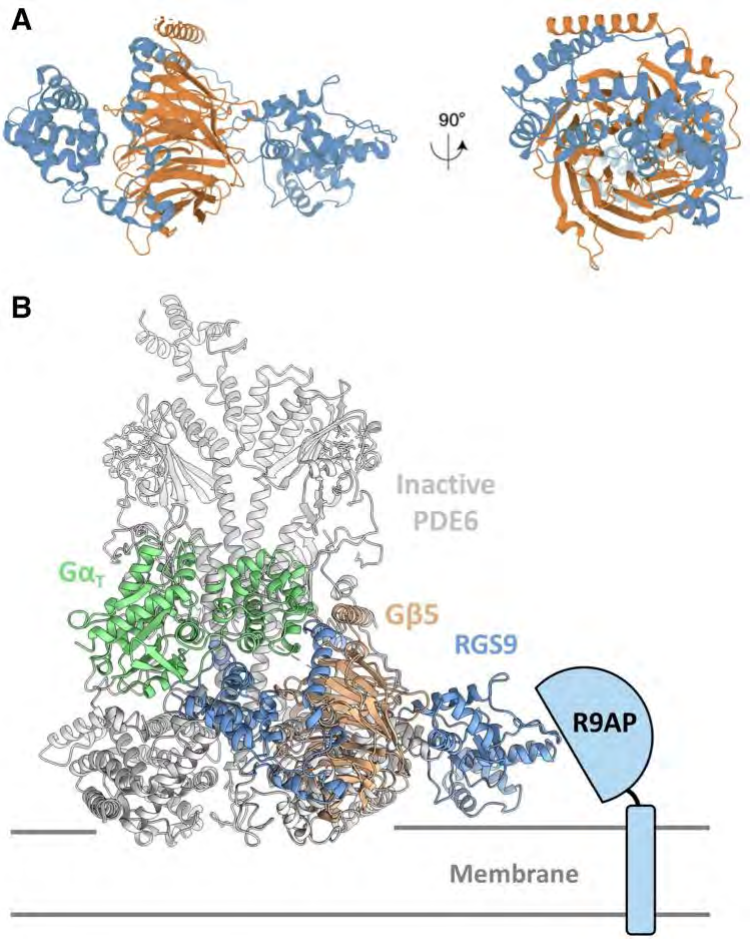


**Figure 11**. Structure for the RGS9 complex. **A.** X-ray crystal structure of RGS9 (blue) with Gβ5 (brown), oriented with the membrane at the bottom (PDB 2PBI) from Cheever et al. (2008) created with Mol* (Sehnal, D., Rose, A.S., Kovca, J., Burley, S.K., and Velankar, S. 2018. Mol*: Towards a common library and tools for web molecular graphics MolIVA/EuroVis Proc. doi: 10.2312/molva.20181103), RCSB PDB. **B.** Alignment of the RGS-Gβ5 complex (blue, brown, PDB 2PBI) with the cryo-EM structure of PDE6 (gray, PDB 6MZB) and Tα-subunit (green), based on the X-ray crystal structure of Tα-subunit bound to a fragment of RGS9 (PDB 1FQJ). Adapted from Gao, Y., Eskici, G., Ramachandran, S., Poitevin, F., Seven, A.B., Panova, O., Skiniotis, G., and Cerione, R.A. 2020. Structure of the visual signaling complex between transducin and phosphodiesterase 6. Mol. Cell 80: 237-245, doi:10.1016/j.molcel.2020.09.013 10.1016/j.molcel.2020.09.013, with permission from Elsevier, https://www.sciencedirect.com/journal/molecular-cell.

It might seem that Nature over-engineered rhodopsin, but it is not the case. Stochastic events have an exponential distribution, so thermally isomerized rhodopsins (R') appear as:

$$R' = R_{ttl} (1 - e^{-t/\tau}) \quad (3)$$

which means that even though it takes 400 years for half of the rhodopsin to thermally isomerize, some isomerize rapidly (**Fig. 13A**). Accordingly, in a rod with two hundred million

rhodopsins, there will be on average one thermal isomerization every 1.5 minutes[6,7]. **Figure 13B** shows a recording of a single rod's response to dim flashes. Poisson statistics are obeyed; sometimes the rod does not respond, while at other times it detects a photon, and sometimes it detects two. Once in a while, there is an isomerization of rhodopsin due to thermal activation and the rod gives a "response" even though no photon was absorbed (asterisk in **Fig. 13B**). The spontaneous events do not interfere with vision as long as their rate of occurrence is overwhelmed by the rate of responses arising from photon absorptions. But as the light becomes exceedingly dim, our absolute visual sensitivity is limited by this rate of thermal activation. So, while rhodopsin is incredibly stable, it has not been grossly over-engineered.

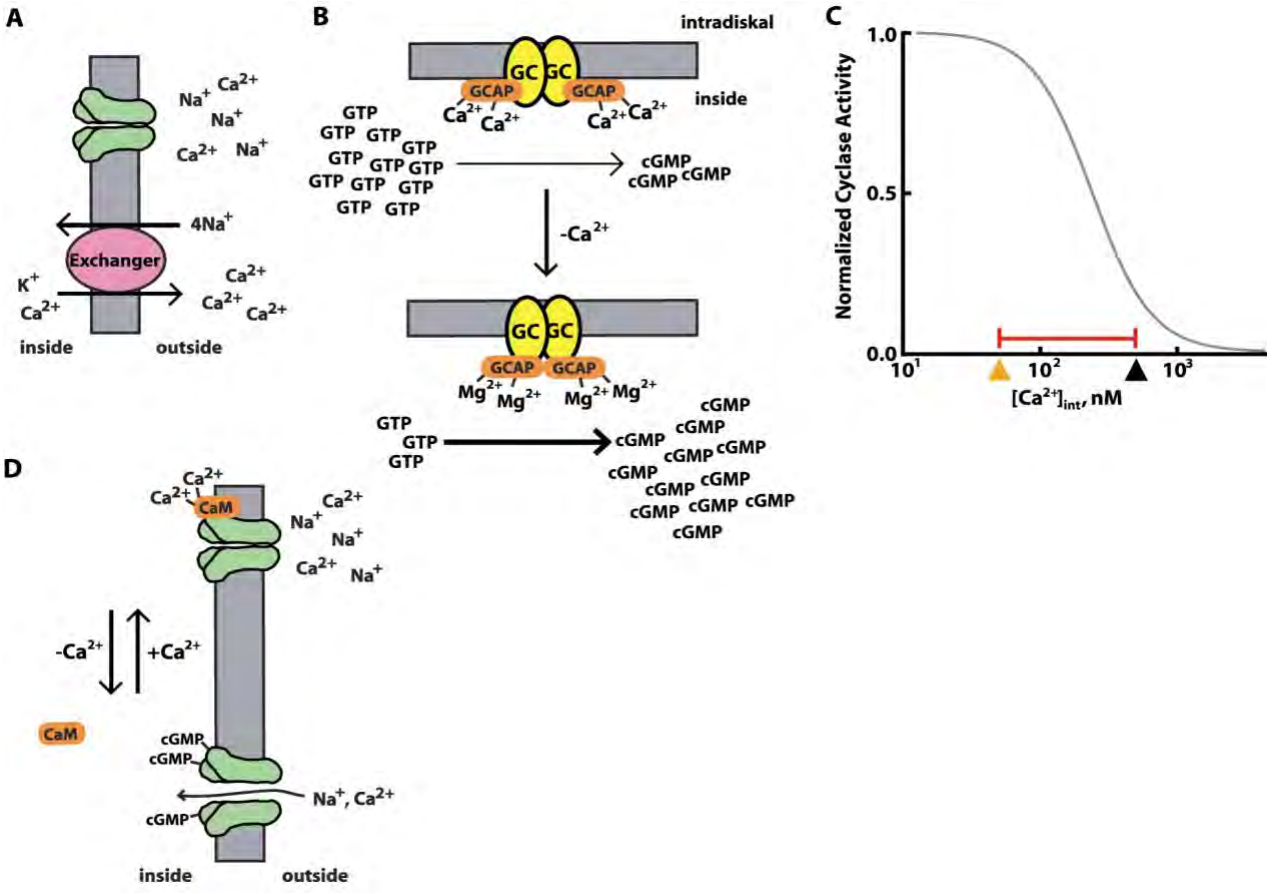


**Figure 12.** $Ca^{2+}$ feedback onto the visual transduction cascade. **A.** $Na^+/K^+,Ca^{2+}$ exchange. In response to light, CNG channels in the outer segment membrane shut, hyperpolarizing the cell. An exchanger in the outer segment couples the removal of a $Ca^{2+}$ to the movement of one $K^+$ and one $Na^+$ down their electrochemical gradients. **B.** Production of cGMP by homodimeric, membrane guanylate cyclases (GCs). GCAPs (guanylate cyclase activating proteins) are $Ca^{2+}$-sensing subunits that inhibit GCs in darkness, when $Ca^{2+}$ levels are high (top). With the light-induced fall in $Ca^{2+}$, $Mg^{2+}$ binds GCAPs in place of $Ca^{2+}$ and GCAPs become stimulators of GCs (bottom). **C.** $Ca^{2+}$-dependence of GC activity. At dark-adapted $Ca^{2+}$ levels (black arrowhead), GC operates at a low level, but visual transduction causes a drop in $Ca^{2+}$ to lower levels (orange arrowhead) and elicits a GCAP-mediated increase in GC activity according to a Hill function: $A = (A_{max} - A_{min})/(1 + ([Ca^{2+}]/K_{m\ Ca})^n) + A_{min}$, where A is GC activity, $K_{m\ Ca}$ is 240 nM, and n is 2. **D.** Cyclic nucleotide-gated channel. Re-opening of the channel is affected by $Ca^{2+}$ levels through the activity of calmodulin (CaM). As $[Ca^{2+}]_{in}$ decreases

during the response to light, CaM releases from the channel, causing an increase in the channel's affinity for cGMP. The increased affinity promotes nucleotide binding and channel opening. As $[Ca^{2+}]_{in}$ rises, CaM binds the channel once more and reduces its affinity for cGMP. Illustrations, courtesy of Tomoki Isayama, Massachusetts Eye & Ear Infirmary and Harvard Medical School.

The next component in the phototransduction cascade, transducin, is the most stable G protein known. Random activation, that is spontaneous exchange of GTP for bound GDP, takes hours. Transducin is not nearly as stable as rhodopsin, but there are ten-fold fewer of them in the outer segment than there are rhodopsins. It is further mitigated by the requirement that two transducins with GTP must bind to the PDE before there is any cGMP hydrolysis. To achieve PDE activation, the thermally activated transducins must be near each other and bind to the same PDE. Even after being activated, the average effect of one activated PDE is ten times smaller than that of a single R*.

PDE is noisier still. About one in 5000 PDEs is spontaneously active at any given time, but there are ten-fold fewer PDE than transducins. Nevertheless, at any instant in time, hundreds of PDEs are active in the dark. Most of the time, PDE shuts off quickly and thanks to negative $Ca^{2+}$ feedback on GC activity, the end result is tiny. But once per 1000 s, there is an event that could be mistaken for photon capture. PDE noise serves a critical physiological function, however. In darkness, cGMP is constantly synthesized, so without dark PDE activity, cGMP would accumulate and start to open all of the CNG channels. The rod has a lot of channels with only a small percentage open in darkness. If the rod were to synthesize too much cGMP, many more channels would open and $Na^+$ and $Ca^{2+}$ would deluge the rod. This disastrous situation occurs in some forms of retinal disease, resulting in photoreceptor death and blindness.

The last component of the cascade, the CNG channel, is very, very noisy. Even in saturating cGMP, the channel opens and closes incessantly (**Fig. 13C**). The behavior is a tradeoff related to its cooperativity of cGMP binding, which was useful for amplification. The channel's affinity for cGMP and its probability of opening increase as more cGMP is bound. By the law of microscopic reversibility, cGMP tends to stay bound to the open channel. So for the channel to respond to changes in cGMP concentration, it must revert to the closed state to give the cGMP a chance to unbind. Once the channel is closed, if the concentration of cGMP is high, another cGMP will bind and re-open the channel. But if the concentration of cGMP is low, the channel will stay closed. Thus, channel flicker (noise) ensures a rapid response to a decrease in cGMP.

To minimize the impact of a noisy channel, the rod lowers the channel conductance, i.e., the number of ions that can pass through the channel at a given voltage. Some channels are selective about which ions are allowed to enter, but not the rod channel; it allows passage of $Na^+$, $Ca^{2+}$ and $Mg^{2+}$. All pass through the pore in single file. Sodium ions are well disciplined and march briskly through the pore. In contrast, $Ca^{2+}$ and $Mg^{2+}$ dwell in the pore for a time and block it, before finally passing through. On average, the channel conductance is one hundred times lower in the presence of physiological levels of divalent ions ($Ca^{2+}$ and $Mg^{2+}$). Another feature is that divalent "block" is voltage dependent. The more hyperpolarized the cell, the greater the block. Voltage-dependent block as well as a mild voltage dependence to the gating of the channel have an effect on the current-voltage relation **(Fig. 14C)**. At positive potentials, the driving force for divalent entry is low so there is minimal block and the current-to-voltage relation is ohmic (proportional to voltage). But in the physiological range of voltages, the driving force for divalent entry gets stronger at more negative voltages causing the relation to flattern. The total

current flows out more readily than it flows in, so the channel is said to be outwardly rectifying. Therefore, over the physiological range of voltages, the change in current is strictly dependent upon the number of channels open. At dim intensities, that feature helps the rod to respond linearly at dim intensities -- the rod counts photons. The reduction in dark current produced by two photons is simply twice that produced by one photon.

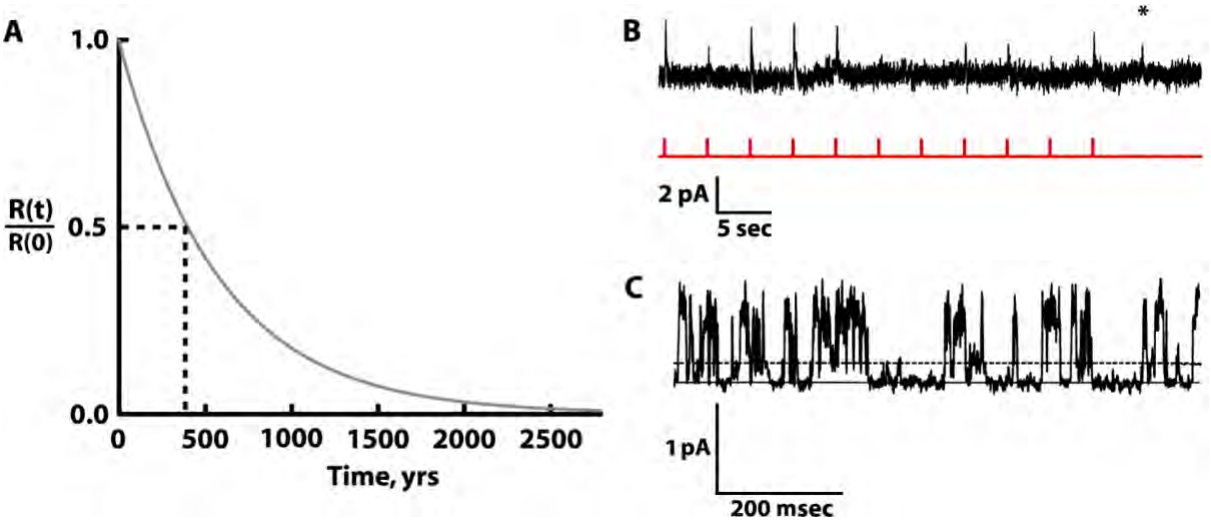


**Figure 13**. Noise in the system. **A**. Exponential decay of rhodopsin in darkness due to thermal isomerization. At 37°C, rhodopsin has a half-life of about 400 years. **B**. Dim flash responses of a mouse rod. The flashes are so dim that not all elicit a response. Sometimes, a "response" appears without a flash (*). The lowermost trace shows the timing of flashes. Figures, courtesy of Tomoki Isayama, Massachusetts Eye & Ear Infirmary and Harvard Medical School. **C**. Current fluctuations of a single CNG channel from a rod in saturating cGMP. The "fuzziness" in the open state results from unresolved transitions back to the closed state (denoted by the continuous horizontal line). Some transitions are to a second activated state marked by a lower peak conductance (dashed line). $V_m$ = +50 mV, with symmetric, low divalent solutions on each side of the membrane. Figure adapted from Taylor, W.R. and Baylor, D.A. 1995. Conductance and kinetics of single cGMP-activated channels in salamander rod outer segments. J. Physiol. (Lond) 483: 567-582, John Wiley & Sons, Inc. © The Physiological Society. https://doi.org/10.1113/jphysiol.1995.sp020607.

The response to a single photon is a small fraction of the maximal, saturating response (**Fig 14A**). Photon absorption is random along the length of the rod (**Fig. 14B**). Photon absorption closes channels in an annulus around the disk containing the R*. The axial expanse of channel closure is narrow, compared to the total outer segment length (**Hyperlink 5: Biophysical modeling**). When two photons are absorbed, it is highly unlikely that both would be absorbed in the same disk. Since each photon produces a local effect that is independent of the response to photons at distant locations, the overall response is twice as large (**Fig. 14D**). With more and more photon absorptions, the effects of individual rhodopsin isomerizations begin to overlap, so there are diminishing returns and the rod response diverges from linearity. The behavior follows a saturating exponential:

$$r/r_{max} = 1\text{-}e^{-ki}, \quad (4)$$

where *i* is flash strength and *k* is a constant equal to the quotient of ln(2) divided by the flash

strength giving rise to a half-maximal response (**Fig. 14D,** gray trace). Bright flashes close all of the channels and saturate the rod ($r/r_{max}$ = 1). Supra-saturating flashes reduce cGMP further, keeping the rod saturated for a longer time before recovering, because more time is needed to re-synthesize cGMP to a level that reopens the channels.

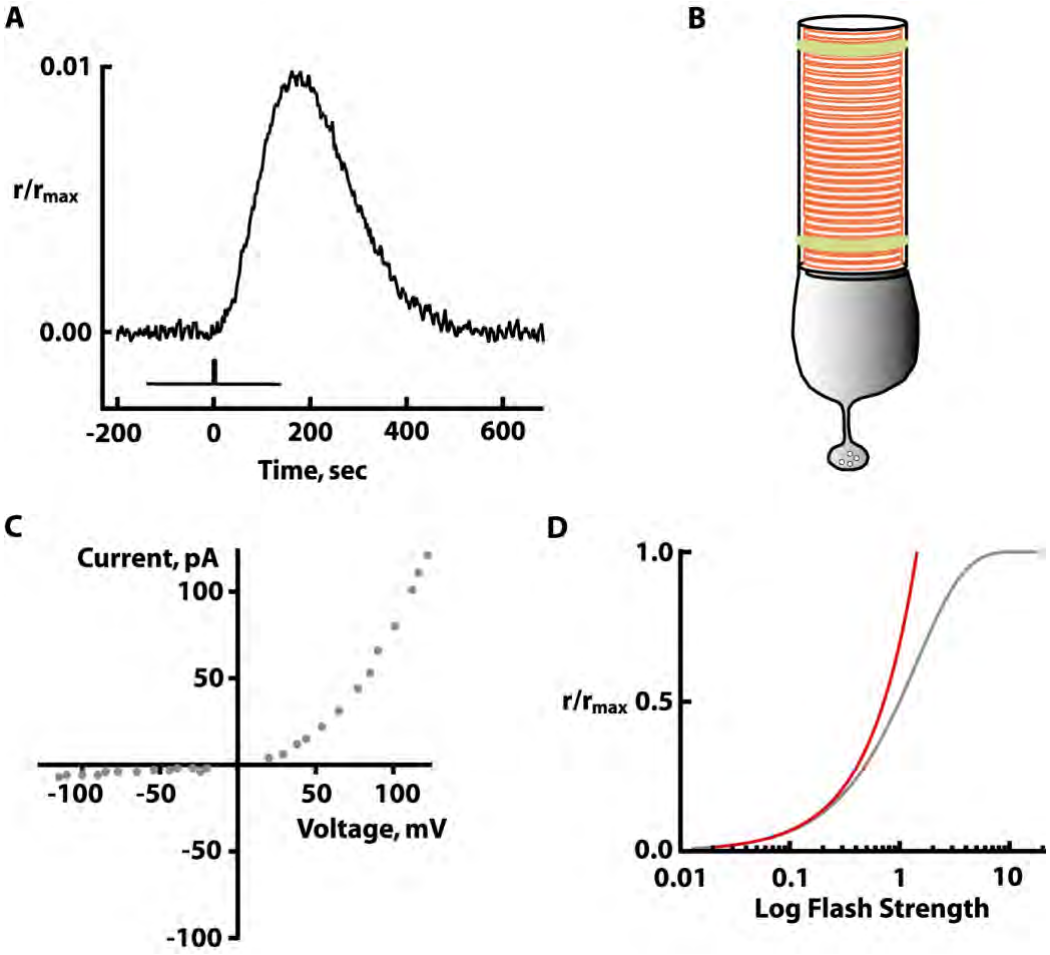


**Figure 14.** Absorption of 2 photons. **A.** Primate single photon response. The response to a single photon is presented as a fraction of the saturating response amplitude (14 pA for this rod). The line beneath the response shows the timing of the flash. Figure, courtesy of Julie Schnapf, University of California San Francisco. **B.** Spatial distribution of rhodopsin photoisomerization. Two photons are unlikely to be absorbed in the same disk, and therefore produce localized closure of CNG channels independent of each other (green annuli). **C.** Current-voltage relations. The ohmic or linear behavior at positive voltages becomes outwardly rectifying at physiologically relevant voltages, meaning that in this range the dark current is nearly independent of membrane potential. Measurements were made on a membrane patch excised from a toad rod outer segment with symmetric monovalent solutions plus 1 mM $Ca^{2+}$ and 1.6 mM $Mg^{2+}$ on the extracellular face, but zero divalents, 0.15 mM EDTA and 1 mM cGMP on the intracellular face. Figure, courtesy of Gary Matthews, State University of New York at Stony Brook. **D.** Stimulus-response relation for a mouse rod. The response to multiple photon absorptions can be described by a saturating exponential function (gray trace). A linear relation between response and flash strength (red trace) is shown for comparison. The

two plots diverge when photon absorptions start to close CNG channels in overlapping annuli of plasma membrane. Figure, courtesy of Tomoki Isayama, Massachusetts Eye & Ear Infirmary and Harvard Medical School.

In summary, the rod is dedicated to producing a highly amplified, reproducible response to photons on a quiet background. The price? Amplification takes time and that imposes a limit on how fast we can see. The motion picture industry takes advantage of that operating characteristic: movies are a series of still shots zipping by faster than we can see them individually. Noise is minimal but not nonexistent. Rhodopsin sits at the top of the cascade and is the quietest component but it ultimately imposes a limit on how sensitive our rods can be. Noisiness in cascade components increases as we move downstream, but the effects have important physiological uses[8].

For further information, we recommend:

Fain, G.L. 2020. Sensory Transduction 2nd edition. Oxford University Press, New York.

Hofmann, K.P. and Lamb, T.D. 2022. Rhodopsin, light-sensor of vision. Prog. Ret. Eye Res. doi: 10.1016/j.preteyeres.2022.101116.

Kawamura, S. and Tachibanaki, S. 2022. Molecular bases of rod and cone differences. Prog. Ret. Eye Res. 90: 101040. doi: 10.1016/j.preteyeres.2021.101040.

Lamb, T.D. 2022. Photoreceptor physiology and evolution: cellular and molecular basis of rod and cone phototransduction. J. Physiol. (Lond) 600: 4585-4601.

Wensel, T.G. 2024. Biochemical cascade of phototransduction. In Adler's Physiology of the Eye 12th edition. P.L. Kaufman, A. Alm, L.A. Levin, S.F.E. Nilsson, J. Ver Hoeve, and S. Wu, editors. Elsevier, NY.

**Acknowledgments**
This tutorial is dedicated to Denis Baylor (1940-2022), whose seminal contributions greatly advanced our understanding of visual transduction. We will treasure his guidance and friendship always. We thank numerous other colleagues for discussions and for providing figures and videos, T. Isayama and A.L. Zimmerman for contributing to an earlier posting of the tutorial, and W. Baehr, E. Bullitt, H. Hamm, T. Isayama, for helpful comments. Supported by NEI EY031702, but the authors are solely responsible for the contents herein, which do not necessarily represent the official views of the National Institutes of Health.

**Notes to instructors**

**1** We like to start the lecture on visual transduction with a brief exercise. Divide the class into groups of 3-4 students. Ask students to imagine that they live in a remote mountain village (**Fig. 15**). All citizens of the village are members of three-person, early warning teams whose job is to stand outside whenever it starts to snow and count the number of snowflakes that land on a calibrated plot of land. If the rate of snowflakes falling on that plot of land should surpass a certain threshold, the team sounds an alarm to evacuate the village because it is likely that there will be an avalanche and in doing so, hundreds of lives will be saved. If there are too many

false positive errors, fellow villagers will not be happy about abandoning what they were doing to be sent out into the cold for no reason. Next time, they might not leave and hundreds of lives may be lost needlessly.

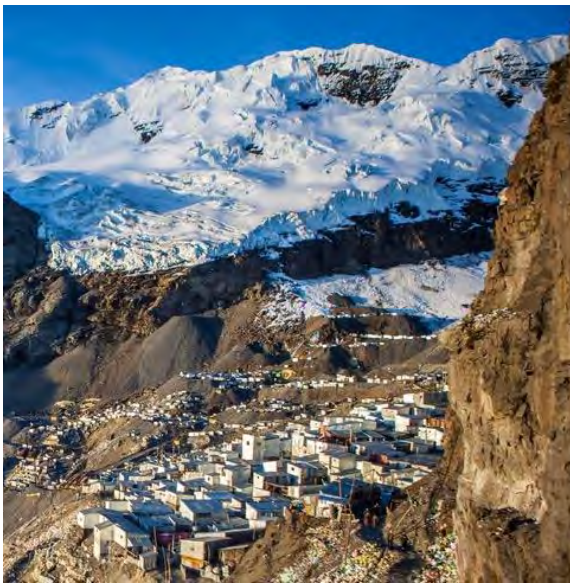

**Figure 15.** Remote mountain village. Photograph, courtesy of Walker Dawson.

Task the groups with discussing: i) reasons the job of counting snowflakes is challenging (what might complicate or interfere with the task?), ii) ways to optimize performance (what could be done to make counting snowflakes easier or to increase accuracy?). After 3 minutes, reconvene the class for a larger discussion. Ask a spokesperson from each group to give one idea from their list of discussion points. Assign the ideas to one of five categories, listed below. This could be done on the board as students give verbal responses. Alternately, this exercise could be given as a pre-class assignment and the instructor could assemble and categorize responses prior to class.

Write the categories in the following order: i) **dedication** - no matter how important, no matter the pay, there are many other things that are more enjoyable and because the disastrous event is so rare, it is difficult to stay focused on such a monotonous task, ii) **sensitivity/amplification** - individual snowflakes are so small that it would be useful to magnify (or amplify) them in some way, iii) **timing** - many snowflakes might fall at the same time and at uneven rates that approach the limit of the ability to count them, iv) **reproducibility** - snowflakes might start to melt or stick together, and v) **noise** - it could be difficult to distinguish snowflakes from other small, airborne substances such as ashes or pollen.

**2** Passage of the photon through the outer segment may be likened to running a gauntlet. For centuries, in societies around the world, there was practice in which two rows of tribe members allowed a captive to run between them. The tribe would assault the captive with weapons. Any captive, managing to make it all the way from one end to the other, could go free.

**3** A Stars Wars mnemonic may be helpful: photons battle the forces of evil and shut down the dark current.

**4** Interactive plots can be constructed using this website:

https://www.physiologyweb.com/calculators/hill_equation_interactive_graph

| | | |
|---|---|---|
| Enter parameters: | Maximum velocity ($V_{max}$) | 100% |
| | Michaelis constant ($K_{0.5}$) | 30 μM |
| | Hill coefficient ($n$) | 1 |

Click on Add Plot. Change Hill coefficient ($n$) to 3 and click Add Plot.
Click on triangles (bottom right) to zoom so that 20.1 appears as the maximum on the abscissa.
Click on triangles (top left) to zoom so that 13.42 appears at the top of the ordinate.
Place the cursor on the n=1 curve at [cGMP] = 4 μM (corresponding to the dark adapted condition). Coordinates will appear on the left indicating that the maximum velocity (fraction of channels open) is ~11.7%. Move the cursor to [cGMP] ~ 2 μM. Coordinates change to indicate that the fraction of channels open falls roughly linearly, to ~6.1%.
Change the zoom for the ordinate so that the maximum is 0.3022. Repeat the cursor placement for the n=3 curve. At 4 μM, ~0.23% of the channels are open, whereas at 2 μM, the number of channels open is 0.03%, a drop of 7.7-fold that is nearly exponential, $2^3$ = 8.

**5** A social analogy may help to make the point clear. Suppose it is a nice day and you decide to walk to class instead of taking the bus. You step out of your building and you smell coffee, so you stop to get some at an outdoor cafe. Your buddies come by and you start to throw a frisbee, just for a few minutes. Next thing you know, you missed class. But, what if instead, the second you step outside, a campus security car comes screeching up to the curb, two personnel jump out, throw you in, the car peels out and drops you off at your classroom in 3 minutes. Chances are really good that you will make it to class. It is a question of options and opportunities.

**6** In class, it may be useful to go through the calculations with a student entering the numbers in a calculator. In a rod with two hundred million rhodopsins, how many disappear in one minute?

$$R' = R_{ttl} (1 - e^{-t/\tau})$$

Convert the half-life of 400 years to a time constant (τ) of 577 years, then multiply by: 365 days in a year, 24 hrs in a day and 60 min in an hour to get 303271200 min (roughly 3 x $10^8$ min). Raise e to the (-1 min)/(303271200 min) and multiply by 2 x $10^8$ rhodopsins per rod.

$$R' = R_{ttl} (1 - e^{-t/\tau}) = (2 \times 10^8)(1 - e^{-1/(303271200)}) = 0.66$$

The loss of 0.66 R in 1 min translates to one thermal isomerization per rod every 1.5 min.

**7** Rhodopsin noise can be experienced. Go to a completely darkened room (a blindfold would further guard against stray photons) and wait a few tens of minutes for the eyes to dark adapt. After awhile, flashes begin to appear, scattered randomly in space. These are called phosphenes, sensations produced by the visual system in the absence of light. Considering that the 2 eyes each contain over 100 million rods and that in each rod, a signal is generated every 1.5 min, there should be lots of phosphenes! The retina ought to shimmer! The reason it does not is because Nature has learned a thing or two after millions of years of evolution. The brain does not believe a lone cry of photon in the dark. It only interprets light being present when two or more neighboring rods sense an isomerization at about the same time. As a disclaimer, phosphenes can also be caused by other means such as pharmaceuticals, retinal trauma, some forms of retinal disease, pressure on the eye.

**8** Optional discussion.

1) How might photon capture, and therefore sensitivity, be improved? Hint: Beer-Lambert Law, OD = $\varepsilon cl$.

Answers. As described above, a longer outer segment (increased pathlength, *l*) would improve photon capture. Other solutions found in Nature that increase pathlength include banked retinas, eyeshine, and grouped rods. Banked retinas increase pathlength by arranging rods behind each other to capture photons that successfully passed through the outer segments of preceding rods (**Fig. 16**). *Bajacalifornia drakei* may be the champions of this adaptation with more than 28 banks of rods in their retina. The eyes of some fish, reptiles, mammals (**Fig. 17**) and even spiders have a reflective layer called a tapetum behind the retina in the pigment epithelium or in the choroid that causes light to take a double pass through the outer segments. Reflected light leaving the eye can cause it to glow (eyeshine) in dim light. Some fish group their photoreceptors in a reflective cup lined with guanine crystals to increase photon capture by an order of magnitude (**Fig. 18**). The tradeoff is loss of acuity, but it would be an improvement over the glare accompanying bright light in a retina with a reflective tapetum. Interestingly, some fish have grouped rods and ungrouped rods with very long outer segments, in different areas of the same retina.

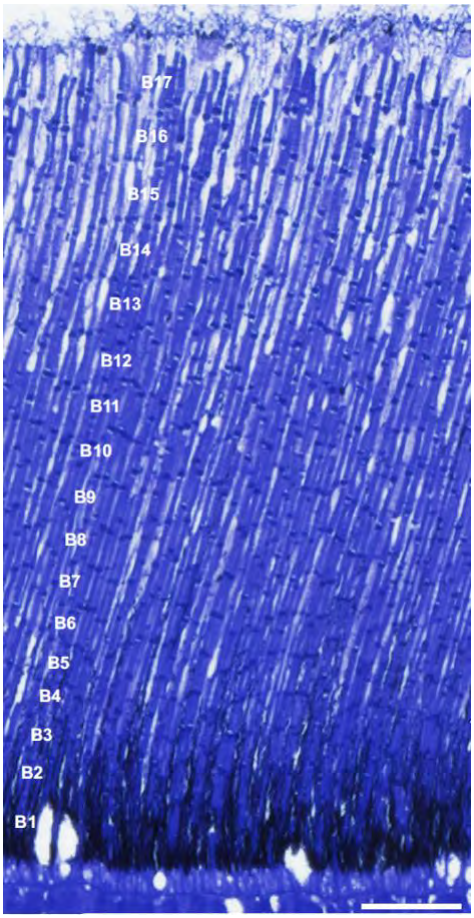


**Figure 16**. Multiple banks of rods of light-adapted *Myrispristis murdjan*. Ventral retina is thickest, with rods arranged into 17 banks. Scale bar 25 μm. Micrograph from de Busserolles, F., Cortesi, F., Fogg, L., Stieb, S.M., Luehrmann, M., and Marshall, N.J. 2021. The visual ecology of Holocentridae, a nocturnal coral reef fish family with a deep-sea-like multibank retina. J. Exp. Biol. 224: jeb233098. doi:10.1242/jeb.233098. Reproduced with permission from The Journal of Experimental Biology.

An alternate solution would be to increase $\varepsilon$, the extinction coefficient of rhodopsin, by adding an auxillary, antenna pigment to sensitize the visual pigment (**Fig. 19**). Rhodopsin already has

a high molecular extinction at $\lambda_{max}$, the wavelength of maximal absorbance, but there is room for improvement at wavelengths for which absorbance is not so high.

**Figure 17**. Eyeshine. From left to right, domestic cat, banded civit from southeast Asia, blue duiker from Africa. Photographs, courtesy of Elina Makino (left), Tim Laman, (middle, right).

Some deep-sea fish rod outer segments have somewhat higher specific absorbance, presumably due to an increase in *c*, rhodopsin concentration within the outer segment. It is not clear how that is achieved. Packing more rhodopsin in the disk membrane would slow response kinetics by exacerbating molecular crowding on the disk surface and reducing collision rates, e.g., between R* and transducin and between transducin and PDE. Surface densities of proteins could be preserved at normal levels if the disk membranes were to be squeezed closer together. But if the disks are too close, proteins on the surface of one disk begin to rub against proteins on the surface of the neighboring disk, again slowing collision rates. Furthermore, it may become increasingly difficult to maintain the thermodynamically unfavorable situation of separating alternating thin layers of lipid and water. The answers await future research.

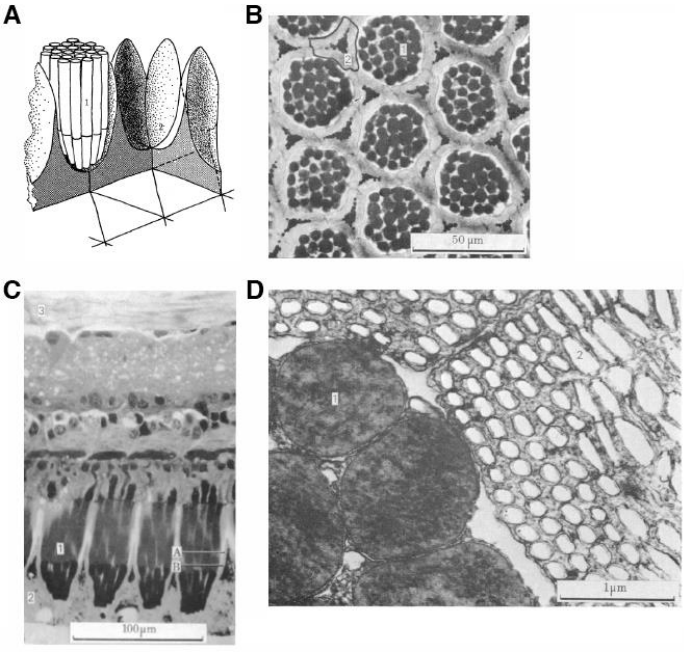


**Figure 18**. Grouped rods. **A**. Schematic of the arrangement of photoreceptors (1) housed within a cup constructed of guanine crystals (2) in the eyes of *Scopelarchus guntheri*. **B,C**. Electron micrographs of retinal cups, each containing ~20 rods. **D**. Higher magnification of rod outer segments and the orientated guanine crystals that form the reflective cup. Cropped and relabeled from Locket, N.A. 1971, Proc. Roy. Soc. Lond. B178: 161-184. Republished with permission of the Royal Society of London.

2) Would humans benefit from these adaptations? What would be the cost?

Answer. Rod outer segments that are 200 μm in length have about seven times more rhodopsin than those of human rods, so thermal isomerizations could pose a problem. How is it feasible in the deep-sea fish? Thermal events are temperature dependent. The half-life for the thermal isomerization of rhodopsin in toads at room temperature is a thousand years which is about two and half times longer than in primate rods at body temperature. Deep-sea fish live in much colder environments; at depths below 200 m, it may only be a few °C. If we extrapolate the temperature dependence of thermal isomerization to their rhodopsin, then the half-life might be around 2500 years, about six times longer than in humans, which makes up for the accumulation of seven times more rhodopsin. So at our elevated body temperature, the noise due to thermal isomerizations would far outweigh any benefit gained from improved photon capture.

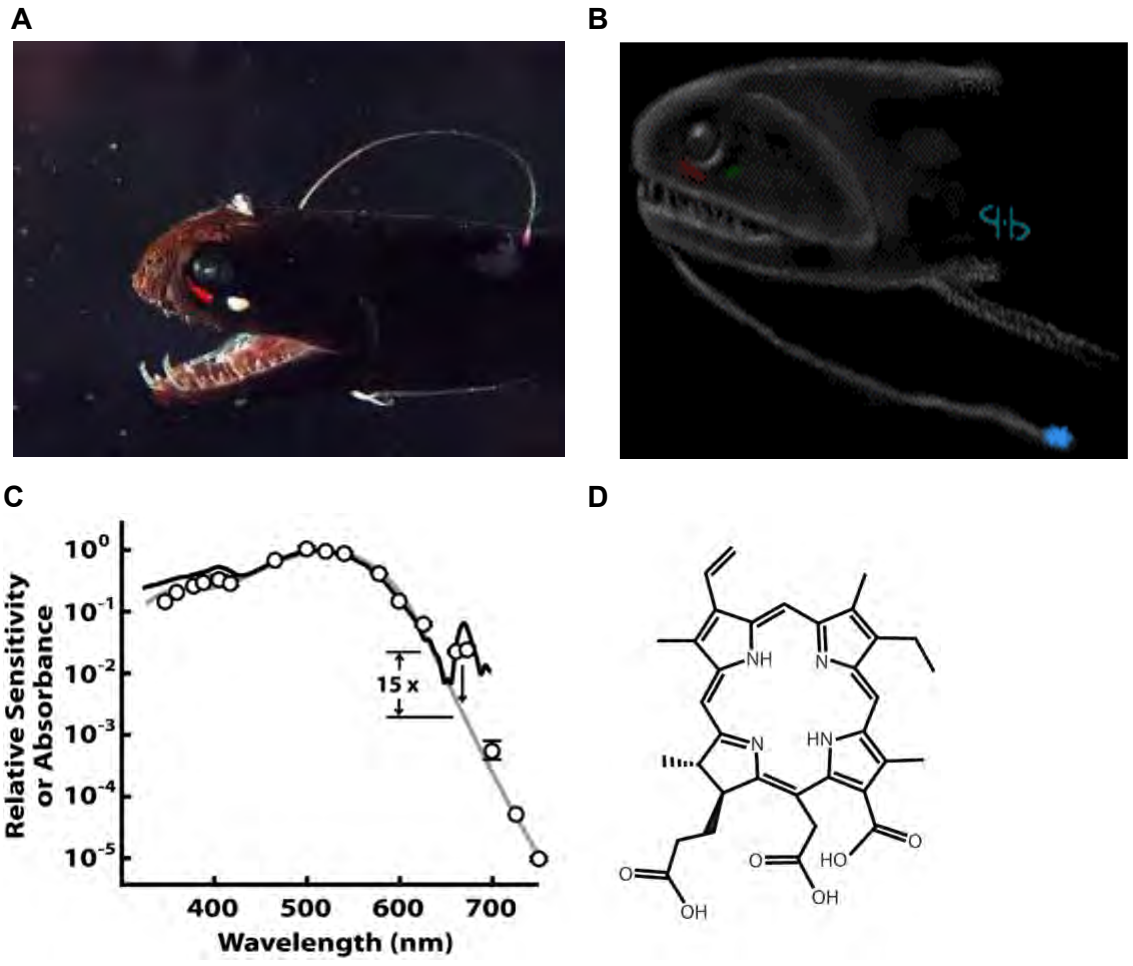


**Figure 19**. Sensitization of visual pigment to long wavelengths. **A,B**. Malacosteid dragonfish have photophores below their eyes that produce light; one set emits blue green bioluminescence and the other, red. (Click on panel **B**) The red serves as a private flashlight because the dragonfish can see the red light whereas most deep-sea dwelling creatures are insensitive to red light. Photograph, courtesy of Tamara Frank, Nova Southeastern University. Illustration, courtesy of Steven Haddock, Monterrey Bay Aquarium Research Institute, https://biolum.eemb.ucsb.edu/. **C**. Artificial sensitization of salamander rhodopsin to red light. Gray line shows the spectral sensitivity of an untreated salamander rod. Circles show the spectral sensitivity after

treatment of the rods with chlorin e6. Black lines show scaled absorbance measurements of separate rods by microspectrophotometry, after treatment with chlorin. Chlorin acts as an antenna pigment that absorbs red light and transfers the energy to rhodopsin, causing it to isomerize as if the rhodopsin had absorbed the photon directly. In this experiment, chlorin treatment increased absorbance and spectral sensitivity to red light by more than tenfold. **D**. Structure of chlorin e6. Chlorin was tested experimentally in salamander rods but is naturally present in dragonfish rods. Bottom panels adapted from Isayama et al., 2016, Nature 443: 649. doi: 10.1038/443649a.

There are other issues associated with metabolic cost. Long outer segments with increased dark current would face energetic demands that are an order of magnitude higher, in order to maintain the ion gradients. In addition, rods turn over their rhodopsin every 10 days in mammals and every 1-2 months in amphibians. In doing so, rods sustain an enormous rate of protein synthesis. Rod are already among the most metabolically active cells in the body and the inability to properly meet metabolic requirements is a major cause of retinal degeneration and blindness. How the fish cope in an environment where food sources may be scarce, is an interesting question.

**Hyperlinks**
H1. Channelrhodopsins and optogenetics
H2. Activations of rhodopsin and transducin
H3. PDE structure and cryo-EM
H4. CNG channel gating
H5. Biophysical modeling

# H1. Channelrhodopsins and optogenetics

Rhodopsin is a 7TM receptor whose structure and function have been studied for decades. In the early 2000's, homologous 7TM proteins were cloned from green (chlorophyte) algae and named "channelrhodopsins" due to their ability to act as ion channels by conducting cations (referred to as cation-conducting channelrhodopsins or CCRs, **Fig. H1-1**) in response to photon capture. These channelrhodopsins covalently link an all-*trans* retinal chromophore at a conserved lysine residue. When a photon is absorbed, all-*trans* isomerizes to 13-*cis* retinal, which leads to opening of the ion channel pore. The function of channelrhodopsins in algae is to guide phototaxis through entry of cations and the resulting membrane depolarization.

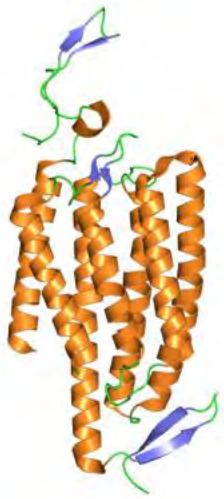

**Figure H1-1**. Crystal structure (PDB 3UG9) of the cation-conducting channelrhodopsin from a chlorophyte.
https://commons.wikimedia.org/wiki/File:3ug9.png
CC BY-SA 3.0
https://en.wikipedia.org/wiki/Channelrhodopsin.

Since then, other channelrhodopsins have been discovered and cloned from blue (cryptophyte) algae; one type conducts cations (CCRs), the other conducts anions (anion-conducting channelrhodopsins or ACRs, **Fig. H1-2**). The physiological function of ACRs in cryptophyte algae remains to be determined.

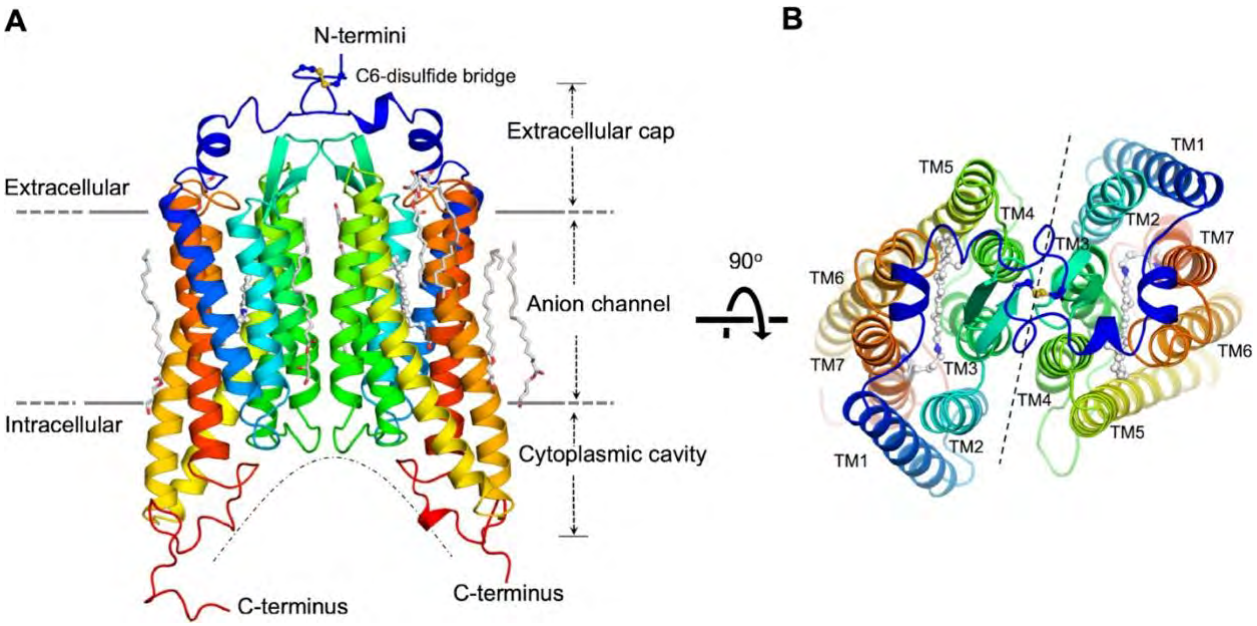

**Figure H1-2**. Crystal structure of *Gt*ACR1 (PDB 6EDQ), the disulfide-crosslinked, homodimeric ACR of the cryptophyte *Guillardia theta* at 2.9 Å. Each subunit has an all-*trans* retinal bound (white balls and sticks). From Li, H., Huang, C.-Y., Govorunova, E.G., Schafer, C.T., Sineshchekov, O.A., Wang, M., Zheng, L., and Spudich, J.L. 2019. Crystal structure of a natural light-gated anion channelrhodopsin. eLife 8: e41741. doi: 10.7554/eLife.41741. 

The development of optogenetics has expanded interest in channelrhodopsins far beyond their function in algae. In this technique, the targeted expression of channelrhodopsins enables selective, photic control of ionic flow and/or enzymatic activity in cells of interest. Karl Deisseroth and his lab members (Deisseroth, 2015) were the first to make neurons "photoactivatable" by expressing a particular channelrhodopsin clone in neurons and then using the appropriate wavelengths of light to stimulate those neurons via activation of that channelrhodopsin.

In the early days of optogenetics, there were many technical hurdles: developing methods for targeted expression of channelrhodopsins in subsets of distinct neurons, reproducibly and dependably stimulating these neurons with light, and carrying out millisecond timescale stimulation while the response of the experimental subject was being measured. It took many years, but now optogenetic techniques have become commonplace in many neuroscience labs. Currently, additional microbial rhodopsins that pump protons or sodium are also being used for neuronal stimulation. Rhodopsins that pump chloride are useful because they can suppress neuronal activity. New and exciting proteins for optogenetics continue to be discovered that expand the optogenetics toolkit. In 2014, a fungal rhodopsin discovered in *Blastocladiella emersonii* (Avelar et al., 2014) was found to be fused to a guanylate cyclase domain which has sequence homology to the membrane guanylate cyclases in rods. In addition, several rhodopsin proteins fused to a phosphodiesterase have been discovered in microbes, the first of which was in the choanoflagellate, *Salpingoeca rosetta* (Yoshida et al., 2017). These rhodopsin fusion proteins allow scientists to control the levels of intracellular signaling molecules optogenetically and have a multitude of implications for the broad field of biology (Mukherjee et al., 2019).

The list of discoveries that have been made using optogenetics is too long to discuss in detail here, but it includes mapping neural circuits and finding out how patterns of activity change in neurodegenerative diseases, understanding and treating cardiac arrhythmias and probing and controlling immune cells (Chen et al., 2022; Zhang et al., 2022). There has even been some success in using a channelrhodopsin to confer light sensitivity to the retina and restore vision to a patient afflicted with a blinding disease caused by degeneration of the retinal photoreceptors (e.g., Sahel et al., 2021).

**Return to Tutorial**

**References**

Avelar, G.M., Schumacher, R.I., Zaini, P.A., Leonard, G., Richards, T.A., and Gomes, S.L. 2014. A rhodopsin-guanylyl cyclase gene fusion functions in visual perception in a fungus. Curr. Biol. 24: 1234–1240.

Chen, B., Cui, M., Shi, P., Wang, H., and Wang, F. 2022. Recent advances in cellular optogenetics for photomedicine. Adv. Drug Deliv. Rev. 188: 114457.

Deisseroth, K. 2015. Optogenetics: 10 years of microbial opsins in neuroscience. Nat. Neurosci. 18: 1213-1225.

Li, H., Huang, C.-Y., Govorunova, E.G., Schafer, C.T., Sineshchekov, O.A., Wang, M., Zheng, L., and Spudich, J.L. 2019. Crystal structure of a natural light-gated anion channelrhodopsin. eLife 8: e41741.

Mukherjee, S., Hegemann, P., and Broser, M. 2019. Enzymerhodopsins: novel photoregulated catalysts for optogenetics. Curr. Op. Struct. Biol. 57: 118-126.

Sahel, J.-A., Boulanger-Scemama, E., Pagot, C., Arleo, A., Galluppi, F., Martel, J.N., Esposti, S.D., Delaux, A., de Sanit Aubert, J.-B., de Montleau, C., Gutman, E., Audo, I., Duebel, J., Picaud, S., Dalkara, D., Bluin, L., Taiel, M., and Roska, B. 2021. Partial recovery of visual function in a blind patient after optogenetic therapy. Nat. Med. 27: 1223-1229.

Yoshida, K., Tsunoda, S.P., Brown, L.S., and Kandori, H. 2017. A unique choanoflagellate enzyme rhodopsin exhibits light-dependent cyclic nucleotide phosphodiesterase activity. J. Biol. Chem. 292: 7531−7541.

Zhang, H., Fang, H., Liu, D., Zhang, Y., Adu-Amankwaah, J., Yuan, J., Tan, R., and Zhu, J. 2022. Applications and challenges of rhodopsin-based optogenetics in biomedicine. Front. Neurosci. 16: 966772.

# H2. Activations of rhodopsin and transducin

Starting with X-ray crystal structures of rhodopsin, metarhodopsin, activated opsin and transducin, as well as that of the β2 adrenergic receptor bound to $G_s$, double electron-electron resonance (DEER) measurements of residue separations and considerations of surface interaction energies were used to construct a model for the sequence of events involved in the photoexcitation of rhodopsin and its subsequent interaction with transducin, the G protein in photoreceptors, that leads to the release of bound GDP from transducin (**Movie H2-1**).

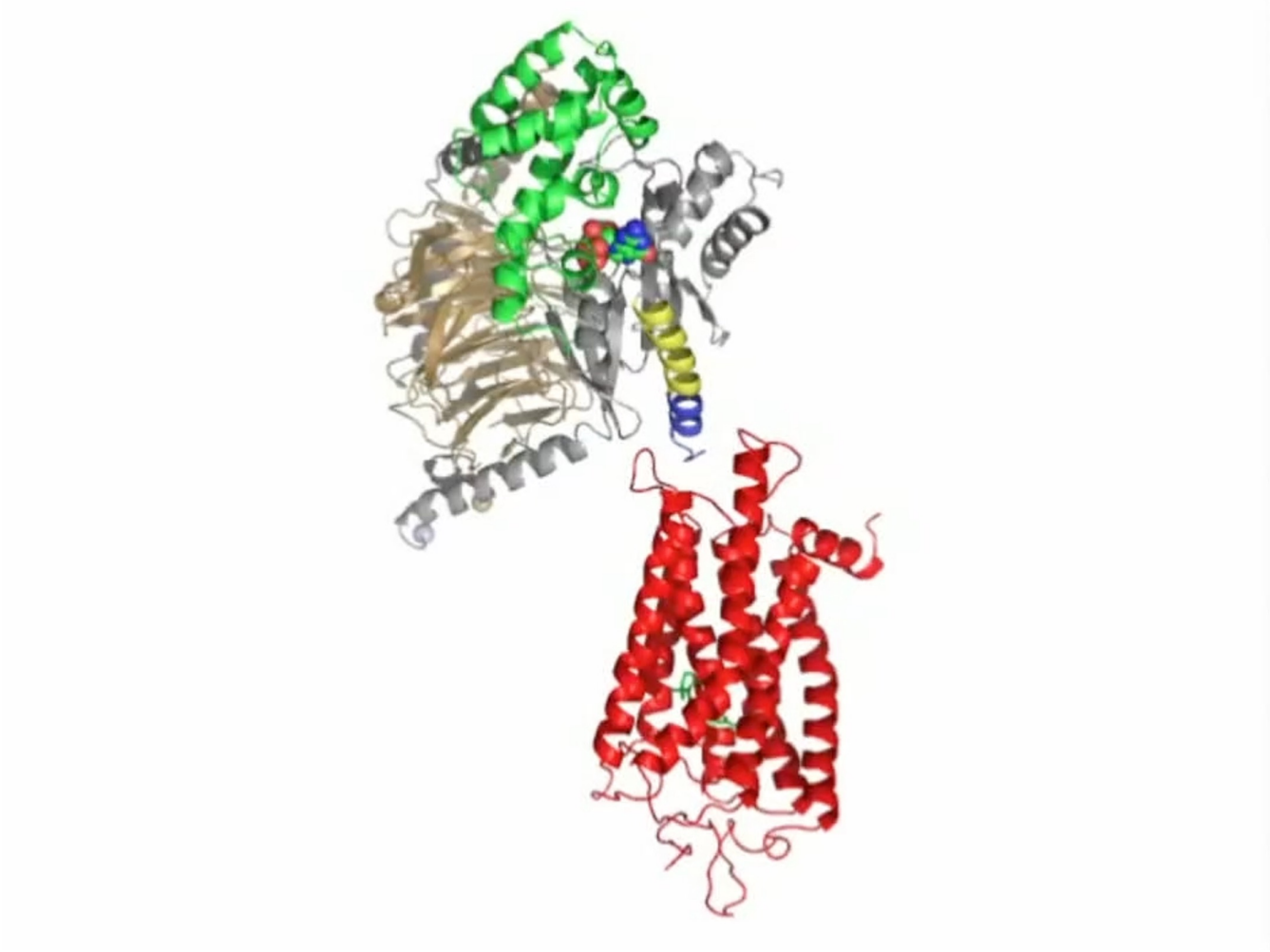

**Movie H2-1**. Dynamics of transducin activation. (Click on image) Photon absorption by the 11-*cis* retinal (green stick structure surrounded by red helices in rhodopsin) isomerizes it to the all-*trans* conformation. Shifts in the opsin/retinal interactions result in a color change shown here as rhodopsin changing from red to gold. In actuality, retinal changes color, not opsin. But because it is difficult to even see the retinal, the artistic freedom taken in showing a color change in opsin is most welcome. As the all-*trans* retinal pushes on its opsin container, the helices splay to open a crevice at the top. Transducin pokes its $\alpha$5 helical finger in and opens its mouth. Rhodopsin grabs the helical finger and in surprise, transducin loses the GDP in its mouth. Rhodopsin, red; photoactivated rhodopsin, gold; $\alpha$5 helix of T$\alpha$, yellow/blue; helical domain of T$\alpha$, green; GTPase domain of T$\alpha$, gray; T$\beta$, brown; T$\gamma$, black; GDP, colored balls; retinal, green stick figure. Simulation, courtesy of Heidi Hamm, Vanderbilt University.

In the DEER approach, pairs of cysteines were introduced into the G protein $\alpha$-subunit at desired locations so that thiol-specific nitroxide spin labels could be attached. All other cysteines were removed. Electron paramagnetic resonance was then probed on frozen samples to determine intramolecular separations in the tens of Angstrom range (Alexander et al., 2014).

**Return to Tutorial**

**References**

Alexander, N.S., Preininger, A.M., Kaya, A.I., Stein, R.A., Hamm, H.E., and Meiler, J. 2014. Energetic analysis of the rhodopsin-G-protein complex links the $\alpha$5 helix to GDP release. Nat. Struct. Mol. Biol. 21: 56-63.

# H3. PDE structure and cryo-EM

The structures of many membrane proteins have not yet been determined because of the difficulty in generating crystals of sufficient size and quality for X-ray diffraction analysis. Cryo-electron microscopy provides an alternative approach that has been applied successfully in the case of the cGMP phosphodiesterase of rods (Gulati et al., 2019). Purified protein prepared from bovine rod outer segments was spread on a grid that had a thin coat of carbon with holes, and rapidly frozen. Tens of thousands of images were captured by transmission electron microscopy from sample within the holes. Because there is only ice and sample over the holes in the grid, these images are 2-dimensional (2D) projections of randomly oriented PDE. Several hundred thousand particles grouped according to 2D profile provided distinct views of the PDE, and these grouped particles were used to produce class averages (**Fig. H3-1**).

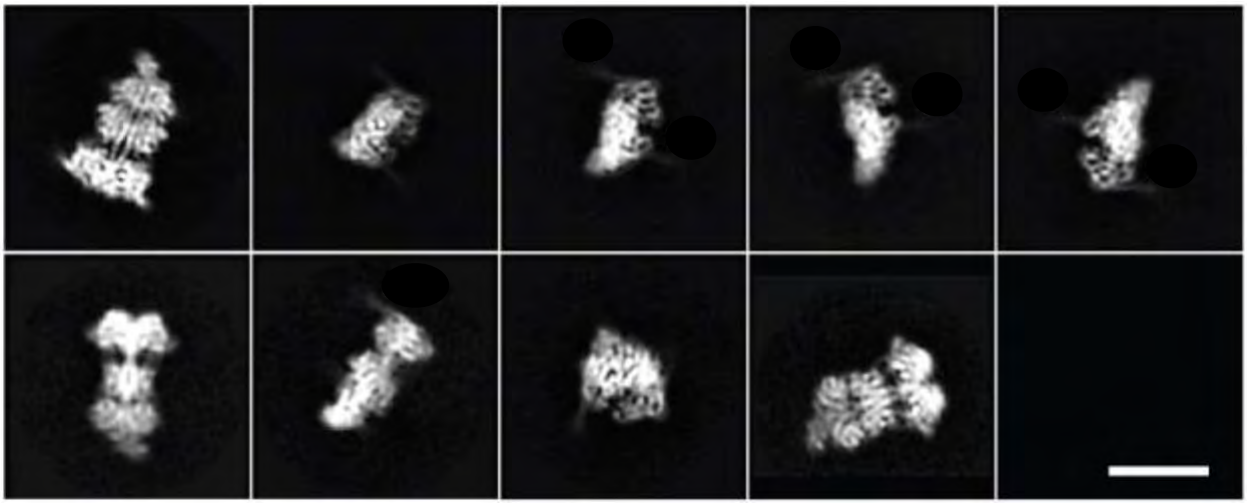

**Fig. H3-1**. Sampling of 2D class averages of PDE$\alpha\beta\gamma\gamma$. Scale bar, 10 nm. From Gulati, S., Palczewski, K., Engel, A., Stahlberg, H., and Kovacik, L. 2019. Cryo-EM structure of phosphodiesterase 6 reveals insights into the allosteric regulation of type I phosphodiesterases. Sci. Adv. 5: eaav4322. doi: 10.1126/sciadv.aav4322. CC BY-NC 4.0 International.

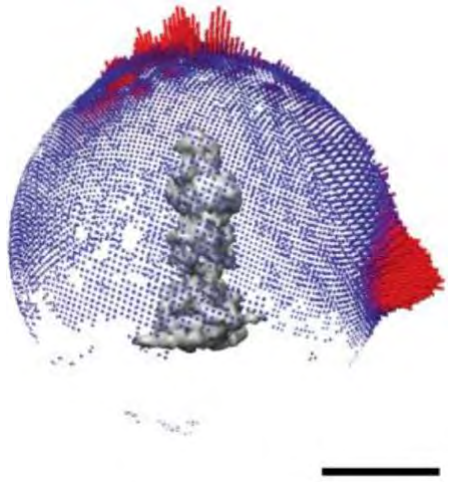

**Fig. H3-2**. Angular distribution of particles used to construct the 3D model (gray). High particle numbers are highlighted in red, lower particle numbers are plotted in purple. Scale bar, 5 nm. Gulati, S., Palczewski, K., Engel, A., Stahlberg, H., and Kovacik, L. 2019. Cryo-EM structure of phosphodiesterase 6 reveals insights into the allosteric regulation of type I phosphodiesterases. Sci. Adv. 5: eaav4322. doi: 10.1126/sciadv.aav4322. CC BY-NC 4.0 International.

2D class averages are 2D projections of the PDE, each from a different orientation. The best class averages were used for further processing. Each class average was oriented with respect to all other classes in order to build 3D models (**Fig. H3-2**) that were then refined, taking into account predictions of secondary structure (**Figs. H3-3, 4**).

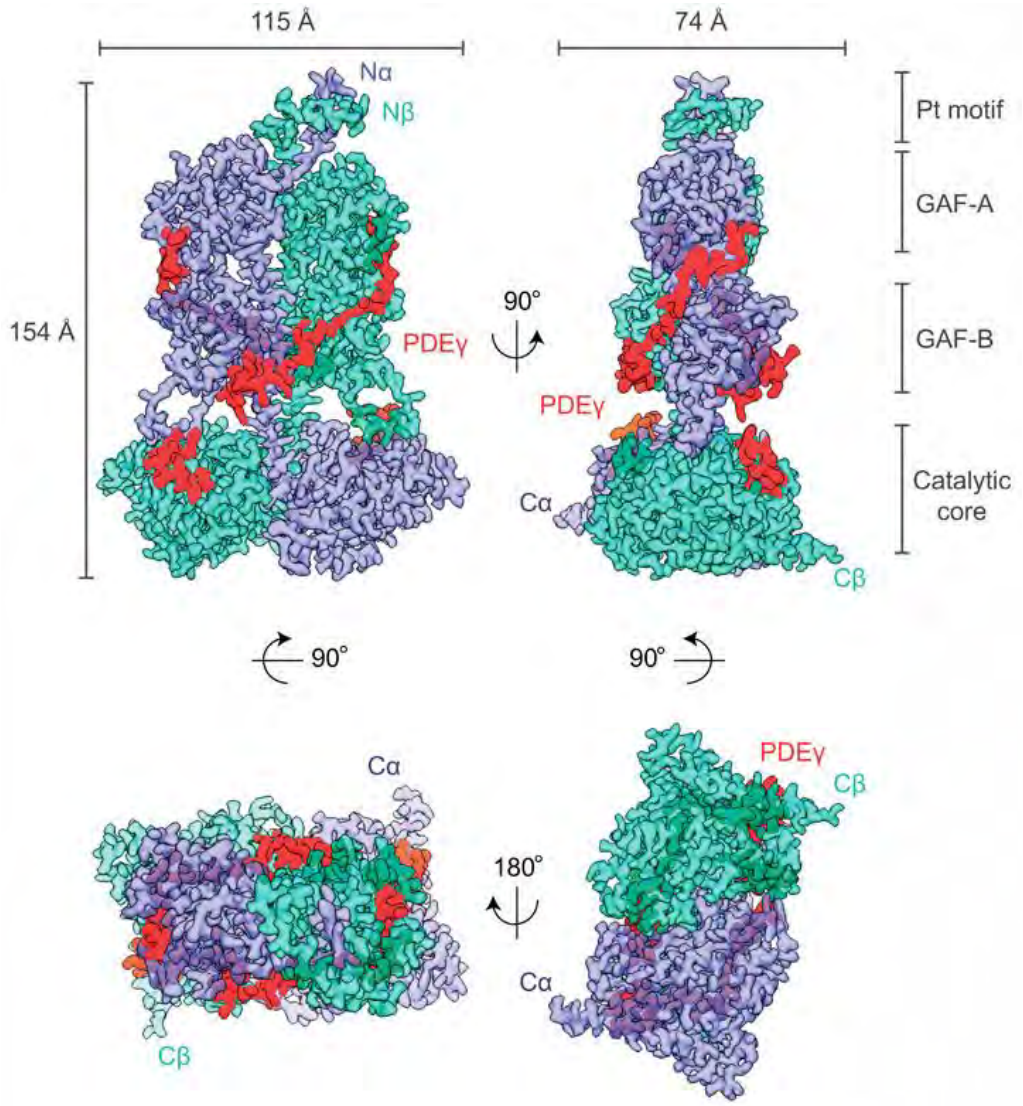


**Fig. H3-3**. Cryo-electron density map of PDE at a resolution of 3.4 Å. PDE is a ternary complex, consisting of two phosphohydrolase catalytic subunits, PDEα (purple) and PDEβ (cyan), each bound with an inhibitory PDEγ (red) subunit. PDE is attached to the membrane by its catalytic core domains. Gulati, S., Palczewski, K., Engel, A., Stahlberg, H., and Kovacik, L. 2019. Cryo-EM structure of phosphodiesterase 6 reveals insights into the allosteric regulation of type I phosphodiesterases. Sci. Adv. 5: eaav4322. doi: 10.1126/sciadv.aav4322. CC BY-NC 4.0 International.

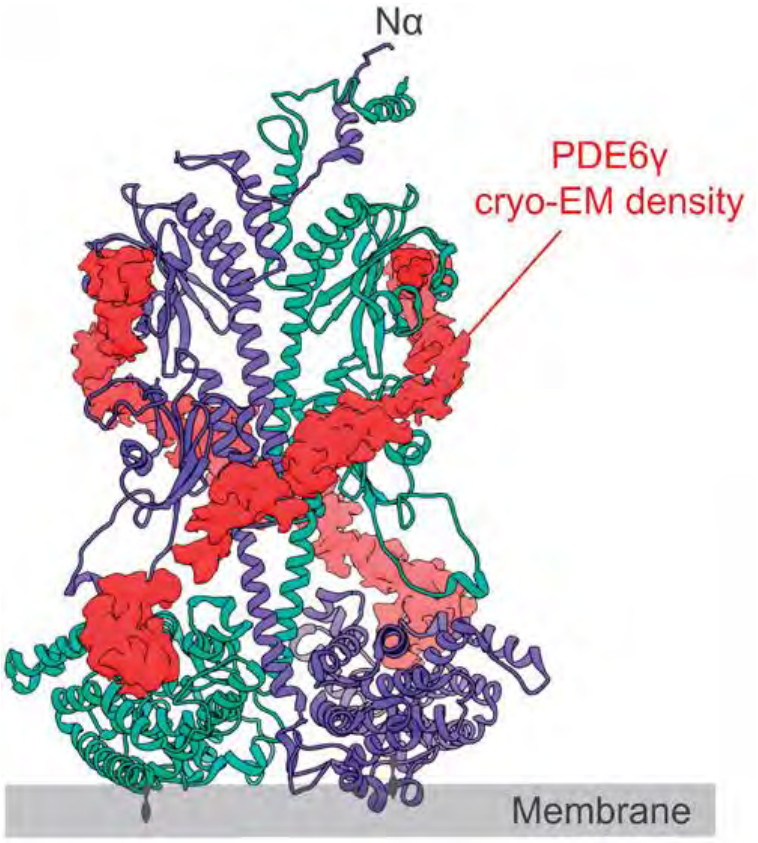


**Fig. H3-4**. Richardson diagram of PDEα (purple) and β (cyan) catalytic subunits with inhibitory γ-subunits (red) shown as density maps from cryo-EM data. Gulati, S., Palczewski, K., Engel, A., Stahlberg, H., and Kovacik, L. 2019. Cryo-EM structure of phosphodiesterase 6 reveals insights into the allosteric regulation of type I phosphodiesterases. Sci. Adv. 5: eaav4322. doi: 10.1126/sciadv.aav4322. CC BY-NC 4.0 International.

The PDEγ-subunits stabilize the open-state, active conformation of the PDEβα heterodimer. However, they also block cGMP molecules from entering the substrate binding sites in the phosphohydrolase domains of the PDEα- and β-subunits, located adjacent to the membrane. The recently determined cryo-EM structure of PDE with active transducins ($G\alpha_T$-GTPs) attached revealed how the latter pry open the PDEγ "doors," to allow cGMP access for hydrolysis (**Fig. H3-5**).

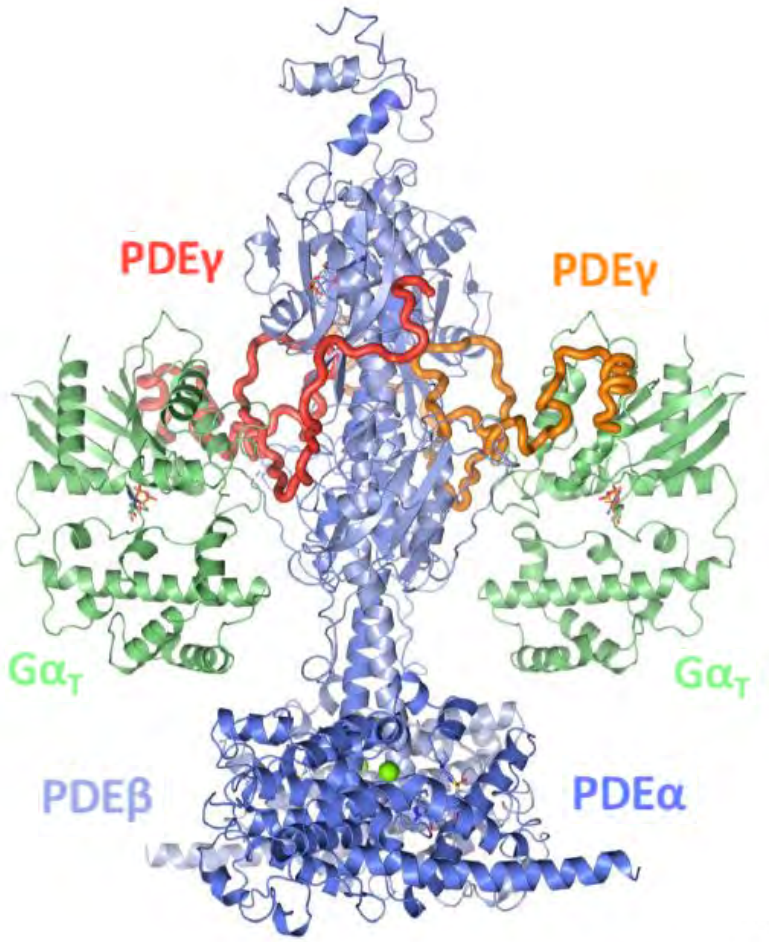


**Fig. H3-5**. Cryo-EM structure of active PDE with 2 activated transducins (G$\alpha_T$ -GTPs) bound. Adapted from Gao, Y., Eskici, G., Ramachandran, S., Poitevin, F., Seven, A.B., Panova, O., Skiniotis, G., and Cerione, R.A. 2020. Structure of the visual signaling complex between transducin and phosphodiesterase 6. Mol. Cell 80: 237-245, doi:10.1016/j.molcel.2020.09.013 10.1016/j.molcel.2020.09.013, with permission from Elsevier, https://www.sciencedirect.com/journal/molecular-cell.

**Return to Tutorial**

**References**

Gao, Y., Eskici, G., Ramachandran, S., Poitevin, F., Seven, A.B., Panova, O., Skiniotis, G., and Cerione, R.A. 2020. Structure of the visual signaling complex between transducin and phosphodiesterase 6. Mol. Cell 80: 237-245.

Gulati, S., Palczewski, K., Engel, A., Stahlberg, H., and Kovacik, L. 2019. Cryo-EM structure of phosphodiesterase 6 reveals insights into the allosteric regulation of type I phosphodiesterases. Sci. Adv. 5: eaav4322. doi: 10.1126/sciadv.aav4322.

## H4. CNG channel gating

The CNG channel of rods is a heterotetramer, consisting of 3 CNGA1 and 1 CNGB1 subunits. The secondary structure of each subunit bears a striking similarity to voltage-gated $K^+$ channels except for its large, intracellular cGMP binding domain. There are 6 transmembrane helices (S1-6): S1-S4 make up a voltage-sensing domain, although the rod channel is only weakly voltage dependent, while S5-6 along with an additional short helix (PH) line the pore and comprise the gate. It is now clear that the CNG channel belongs to a Kv channel superfamily that also includes hyperpolarization-activated CNG channels (HCN) and ether-à-go-go type channels (KCNH). High resolution structures that have been resolved for other members of the superfamily including several that bind cyclic nucleotides provided a crude structural map for the rod channel (**Fig. H4-1**).

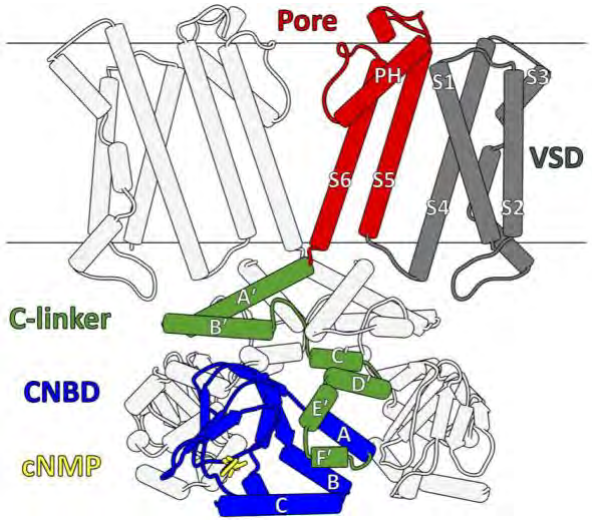


**Fig. H4-1**. Side view of the CNG channel, showing 2 of the 4 subunits. Voltage sensing domain (VSD: S1-4) in gray, pore forming segments (S5, P-helix, S6) in red, C-linker segment with helices A'-F' in green, cyclic nucleotide binding domain (CNBD) with its short $\alpha$ helices A-C and $\beta$ sheets in blue, cyclic nucleotide in yellow. From James, Z.M., and Zagotta, W.N. 2018. Structural insights into the mechanisms of CNBD channel function. J. Gen. Physiol. 150: 225-244. doi: 10.1085/jgp.201711898. License: CC NC-SA 4.0 International.

In cryo-EM structures of a homomeric channel formed from human CNGA1 subunits, with and without cGMP bound, to 2.9 Å and 2.6 Å resolutions, respectively, the central gate of the channel locates in the middle of the membrane, below the ion selectivity filter (Xue et al., 2021). When cGMPs are bound, the CNBDs collapse around them, contracting the C-linker helices and bringing them closer to the membrane. The C-linkers of each subunit rotate around the pore and twist apart the S6 of each subunit, thereby opening the gate (**Movie H4-1**).

Cryo-EM structures of the native human CNG channel reveal that the CNGB1 subunit confers asymmetric pore opening upon cGMP binding (Xue et al., 2022). Furthermore, the CNGB1 subunit and one of its neighboring CNGA1 subunits may or may not undergo the structural changes that support full opening of the pore. This weak coupling of the CNGB1 subunit to pore opening may underlie the flickery behavior of the CNG channel even in the presence of saturating cGMP.

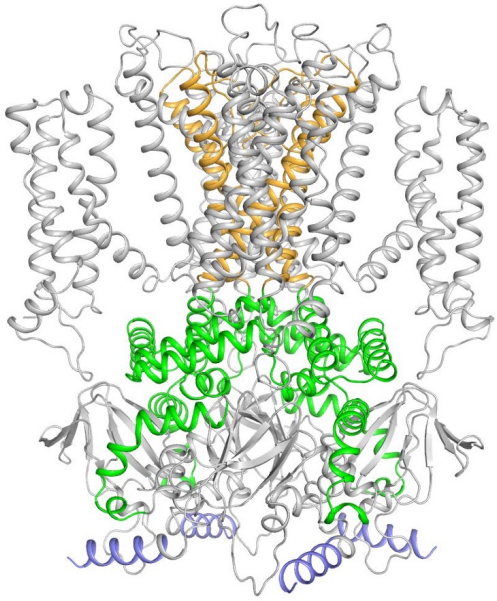

**Movie H4-1**. Model for the gating of a homomeric human rod CNG channel. (Click on image) Transitions between the closed and open states first from a side view and then from the intracellular side. From Xue, J., Han, Y., Zeng, W., Wang, Y., Jiang, Y. 2021. Structural mechanisms of gating and selectivity of human rod CNGA1 channel. Neuron 109: 1302-1313. https://doi.org/10.1016/j.neuron.2021.02.007.

**Return to Tutorial**

**References**

James, Z.M., and Zagotta, W.N. 2018. Structural insights into the mechanisms of CNBD channel function. J. Gen. Physiol. 150: 225-244.

Xue, J., Han, Y., Zeng, W., Wang, Y., Jiang, Y. 2021. Structural mechanisms of gating and selectivity of human rod CNGA1 channel. Neuron 109: 1302-1313.

Xue, J., Han, Y., Zeng, W., and Jiang, Y. 2022. Structural mechanisms of assembly, permeation, gating, and pharmacology of native human rod CNG channel. Neuron 110: 86-95.

# H5. Biophysical modeling

In a landmark achievement, Lamb and Pugh (1992) curated a large database of biochemical and biophysical parameters that were determined experimentally and generated a mathematical model for the activation of phototransduction in rods, linking the interactions of rhodopsin, transducin and PDE to the behavior of CNG channels in the plasma membrane. By treating the aqueous cytosol of the outer segment as a well stirred volume, the model nicely describes the rising phase of a flash response as a delayed ramp (**Fig. H5-1**) with slope proportional to the amplification of the underlying cascade. For saturating flashes,

$$r(t) = 1 - \exp(-0.5\Phi A(t - t_{eff})^2),\ t > t_{eff}$$

where r(t) is the fractional photocurrent response, $\Phi$ is the number of photoisomerizations, $t_{eff}$ is the irreducible delay introduced by the steps prior to CNG channel closure, A is an amplification constant that takes into account, the catalytic power of PDE and the rate of PDE activations. For the single photon response, the model reduces to

$$r(t) \approx 0.5A(t - t_{eff})^2,\ t > t_{eff}.$$

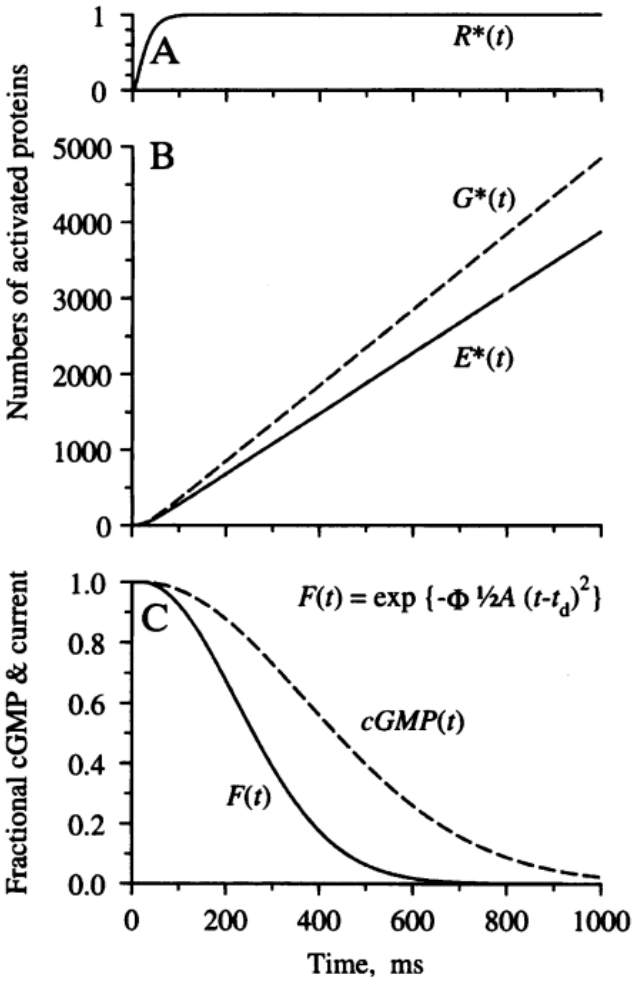


**Fig. H5-1**. Timing of the activation events giving rise to a flash response, as predicted by the Lamb and Pugh model. **A**, **B**. Averaged effects after the photoisomerization of a single rhodopsin (*R**). The activations of transducin (*G* → *G**) and PDE (*E* → *E**) essentially manifest as delayed ramps. **C**. Changes in cGMP and the dark current after a bright, saturating flash. *F(t)* and $t_d$ in their equation correspond to 1-r(t) and $t_{eff}$, above. From Lamb, T.D. 1996. Gain and kinetics of activation in the G-protein cascade of phototransduction. Proc. Natl. Acad. Sci. U.S.A. 93: 566-570. Copyright (1996) National Academy of Sciences, USA.

The model was applied widely and proved to be immensely useful in interpreting quantitatively, the results of physiological experiments on WT and mutant rods. The model was soon expanded to describe the shutoff and recovery phases of flash responses and light adaptation (Pugh & Lamb, 2000).

While the model worked especially well for saturating flashes, there were limitations related to the condition that second messengers diffused with infinite rapidity throughout the aqueous cytosol. Clearly, the single photon response results in localized changes within the outer segment. Furthermore, the outer segment is not homogeneous; responses to photoisomerizations of rhodopsin at the base and the tip differ in size and kinetics (Baylor et al., 1979; Schnapf, 1983; Mazzolini et al., 2015) and there are axial gradients in ion concentrations (Li et al., 2020). A fully space resolved model was developed (Andreucci et al., 2003), taking the clever approach of treating the repeated rows of interdiskal spaces and the outer shell (**Fig. H5-2**) as interconnected surfaces and applying theories of homogenization and concentrated capacity.

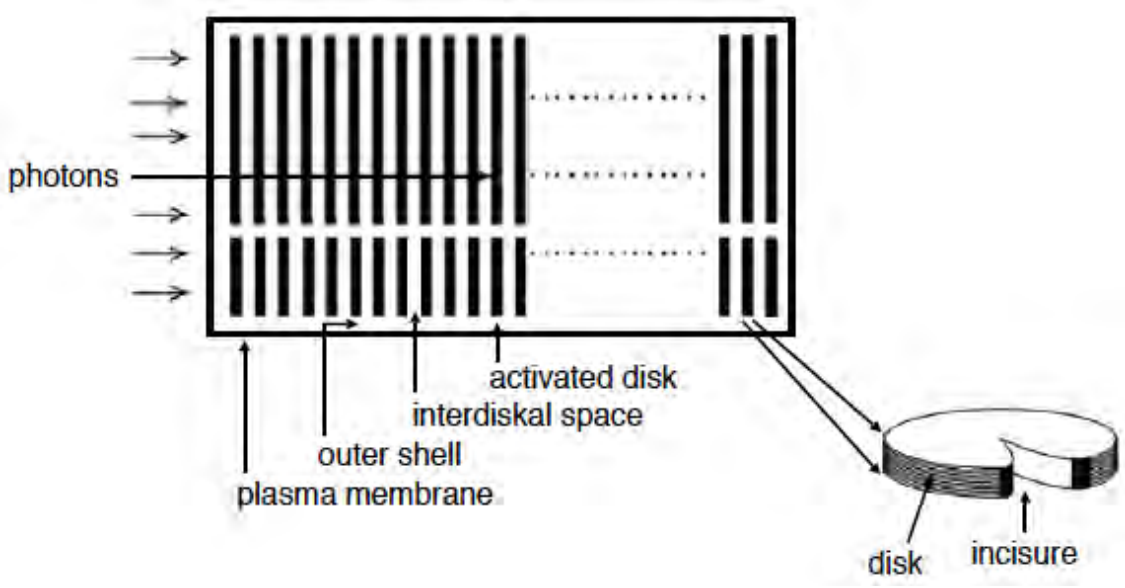


**Fig. H5-2**. Schematic diagram of the rod outer segment. Membranous disks impose barriers to the axial diffusion of soluble substances, e.g., cGMP and $Ca^{2+}$. Cracks or incisures in the disks facilitate axial diffusion. Small mouse rod disks have a single incisure, as shown here. Large amphibian rod disks may have 15-25 incisures.

The model describes the limited, axial spread of activation during a single photon response (**Fig. H5-3**), in general agreement with experimental observations (Caruso et al., 2019). This “next generation” model opens the door for investigating the significance of spatial inhomogeneities within the outer segment and diffusion of soluble substances to single photon response variability and adaptational states. The model can also be applied to exploring the translocation of phototransduction proteins between the inner and outer segments during light adaptation (Sokolov et al., 2002).

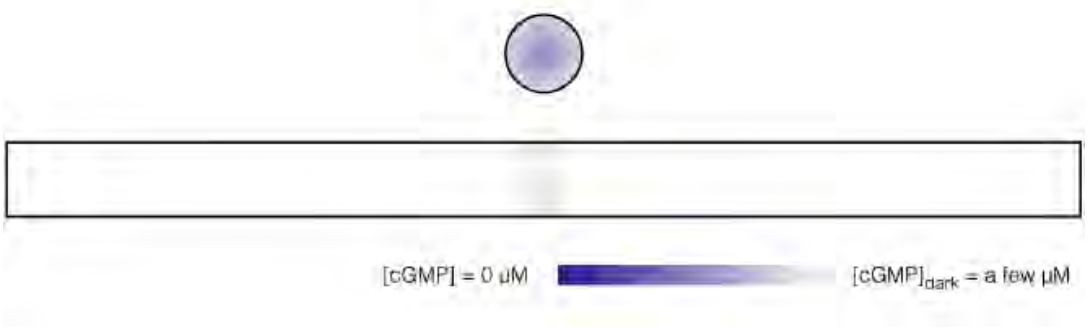


**Fig. H5-3**. Radial and axial gradients of cGMP at the peak of a single photon response, following a rhodopsin photoisomerization in the center of the disk located in the middle of a mouse rod outer segment. Cyclic GMP concentration is represented with a colorimetric scale shown at the bottom: dark purple is the fully depleted cGMP level, white depicts the level of free cGMP present in darkness. Upper panel shows a cross-sectional view of the radial gradient of cGMP depletion in the interdiskal space above the activated disk. The maximal drop in cGMP is in the center where it dips to ~50% the level in darknesss and tapers off to ~25% at the outer shell. Middle panel shows the axial gradient of cGMP in the outer shell. The cGMP depletion falls off steeply along the length of the outer segment, spanning over a hundred disks on each side of the activated disk. The lifetime of R* was taken to be 110 ms, and the diffusion coefficient for cGMP, $D_{cGMP}$, was 120 $\mu m^2\ s^{-1}$. Mouse rod outer segment dimensions were 1.4 μm in diameter x 20 μm in length.

**Return to Tutorial**

**References**

Andreucci, D., Bisegna, P., Caruso, G., Hamm, H.E., and DiBenedetto, E. 2003. Mathematical model of the spatiotemporal dynamics of second messengers in visual transduction. Biophys. J. 85: 1358-1376.

Baylor, D.A., Lamb, T.D., and Yau, K.-W. 1979. The membrane current of single rod outer segments. J. Physiol. (Lond) 288: 589-611.

Caruso, G., Gurevich, V.V., Klaus, C., Hamm, H., Makino, C.L., and DiBenedetto, E. 2019. Local, nonlinear effects of cGMP and $Ca^{2+}$ reduce single photon response variability in retinal rods. PLoS ONE 14: e0225948. https://doi.org/10.1371/journal.pone.0225948.

Lamb, T.D. 1996. Gain and kinetics of activation in the G-protein cascade of phototransduction. Proc. Natl. Acad. Sci. USA 93: 566-570.

Lamb, T.D., and Pugh, E.N. Jr. 1992. A quantitative account of the activation steps involved in phototransduction in amphibian photoreceptors. J. Physiol. (Lond) 449: 719-758.

Lamb, T.D., McNaughton, P.A., and Yau, K.-W. 1981. Spatial spread of activation and background desensitization in toad rod outer segments. J. Physiol. (Lond) 319: 463-496.

Li, Y., Falleroni, F., Mortal, S., Bocchero, U., Cojoc, D., and Torre, V. 2020. Calcium flares and compartmentalization in rod photoreceptors. Proc. Natl. Acad. Sci. USA 117: 21701-21710.

Mazzolini, M., Facchetti, G., Andolfi, L., Proietti Zaccaria, R., Tuccio, S., Treu, J., Altafini, C., Di Fabrizio, E.M., Lazzarino, M., Rapp, G., and Torre, V. 2015. The phototransduction machinery in the rod outer segment has a strong efficacy gradient. Proc. Natl. Acad. Sci. USA 112: E2715-2724.

Pugh, E.N. Jr., and Lamb, T.D. 2000. Phototransduction in vertebrate rods and cones: molecular mechanisms of amplification, recovery and light adaptation. In Handbook of Biological Physics vol 3, D.G. Stavenga, W.J. De Grip, and E.N. Pugh Jr., editors. Elsevier, St Louis, pp. 183-255.

Schnapf, J.L. 1983. Dependence of the single photon response on longitudinal position of absorption in toad rod outer segments. J. Physiol. (Lond) 343: 147-159.

Sokolov, M., Lyubarsky, A.L., Strissel, K.J., Savchenko, A.B., Govardovskii, V.I., Pugh, E.N. Jr., and Arshavsky, V.Y. 2002. Massive light-driven translocation of transducin between the two major compartments of rod cells: a novel mechanism of light adaptation. Neuron 34: 95-106.